Mutagenesis of the Redox-Active Disulfide in Mercuric Ion Reductase: Catalysis by Mutant Enzymes Restricted to Flavin Redox Chemistry†

Mark D. Distefano, Karin G. Au,‡ and Christopher T. Walsh*

Department of Biological Chemistry and Molecular Pharmacology, Harvard Medical School, Boston, Massachusetts 02115

Received June 1, 1988; Revised Manuscript Received September 20, 1988

ABSTRACT: Mercuric reductase, a flavoenzyme that possesses a redox-active cystine, $Cys_{135}Cys_{140}$, catalyzes the reduction of Hg(II) to Hg(0) by NADPH. As a probe of mechanism, we have constructed mutants lacking a redox-active disulfide by eliminating Cys_{135} ($Ala_{135}Cys_{140}$), Cys_{140} ($Cys_{135}Ala_{140}$), or both ($Ala_{135}Ala_{140}$). Additionally, we have made double mutants that lack Cys_{135} ($Ala_{135}Cys_{139}Cys_{140}$) or Cys_{140} ($Cys_{135}Cys_{139}Ala_{140}$) but introduce a new Cys in place of Gly_{139} with the aim of constructing dithiol pairs in the active site that do not form a redox-active disulfide. The resulting mutant enzymes all lack redox-active disulfides and are hence restricted to FAD/$FADH_2$ redox chemistry. Each mutant enzyme possesses unique physical and spectroscopic properties that reflect subtle differences in the FAD microenvironment. These differences are manifested in a 23-nm range in enzyme-bound FAD λ_{max} values, an 80-nm range in thiolate to flavin charge-transfer absorbance maxima, and a ca. 100-mV range in FAD reduction potential. Preliminary evidence for the $Ala_{135}Cys_{139}Cys_{140}$ mutant enzyme suggests that this protein forms a disulfide between the two adjacent Cys residues. Hg(II) titration experiments that correlate the extent of charge-transfer quenching with Hg(II) binding indicate that the $Ala_{135}Cys_{140}$ protein binds Hg(II) with substantially less avidity than does the wild-type enzyme. All mutant mercuric reductases catalyze transhydrogenation and oxygen reduction reactions through obligatory reduced flavin intermediates at rates comparable to or greater than that of the wild-type enzyme. For these activities, there is a linear correlation between log k_{cat} and enzyme-bound FAD reduction potential. In a sensitive Hg(II)-mediated enzyme-bound $FADH_2$ reoxidation assay, all mutant enzymes were able to undergo at least one catalytic event at rates 50–1000-fold slower than that of the wild-type enzyme. We have also observed the reduction of Hg(II) by free $FADH_2$. In multiple-turnover assays which monitored the production of Hg(0), two of the mutant enzymes were observed to proceed through at least 30 turnovers at rates ca. 1000-fold slower than that of wild-type mercuric reductase. We conclude that the Cys_{135} and Cys_{140} thiols serve as Hg(II) ligands that orient the Hg(II) for subsequent reduction by a reduced flavin intermediate.

Mercuric reductase catalyzes the reduction of Hg(II) to Hg(0) by NADPH. This reduction of Hg(II) and the subsequent nonenzymatic volatilization of Hg(0) constitute the mechanism by which bacteria detoxify mercuric salts (Summers, 1986). On the basis of sequence homology (Brown et al., 1983) as well as physical and spectral similarities (Fox & Walsh 1983), mercuric reductase has been classified as a member of the disulfide oxidoreductase family (Williams, 1976). Enzymes in this family all contain a tightly bound flavin cofactor and a redox-active disulfide at the active site. The redox-active disulfide present in glutathione reductase and similar enzymes has been shown to be the actual reductant of external disulfide substrates (Pai & Schulz, 1983). In these cases, the flavin moiety serves only as an electron conduit between NADPH and the redox-active disulfide. For mercuric reductase the function of the enzyme's redox-active disulfide was unclear. It was not known in this case whether the reduced disulfide functions as the actual reductant of Hg(II) or simply as a binding site for the Hg(II). In the latter case reduction would occur by a reduced flavin intermediate, representing a significant mechanistic difference between mercuric reductase and other members of the disulfide oxidoreductase class.

Table I: Active Site Mutants of Mercuric Reductase and Their Overproduction Plasmids

wild-type sequence	mutant sequence	overproduction plasmid
$Cys_{135}Cys_{140}$	$Ser_{135}Cys_{140}$[a]	pPSO2
	$Ala_{135}Cys_{140}$	pKAO1
	$Cys_{135}Ser_{140}$[a]	pPSO3
	$Cys_{135}Ala_{140}$	pKAO2
	$Ala_{135}Ala_{140}$	pMDO3
$Cys_{135}Gly_{139}Cys_{140}$	$Cys_{135}Cys_{139}Ala_{140}$	pMDO2
	$Ala_{135}Cys_{139}Cys_{140}$	pMDO4

[a] Previously reported in Schultz et al. (1985).

To clarify these mechanistic issues and delineate the role of the redox-active disulfide ($Cys_{135}Cys_{140}$), we have used site-directed mutagenesis to construct mutants in the active site of mercuric reductase from Tn*501* (Brown et al., 1983). In an earlier paper we described the properties of two mutants, $Ser_{135}Cys_{140}$ and $Cys_{135}Ser_{140}$, which alter each of the cysteine residues in the redox-active disulfide to serine (Schultz et al., 1985). In this paper we report the construction and characterization of five additional mutants: $Ala_{135}Cys_{140}$, $Cys_{135}Ala_{140}$, $Ala_{135}Ala_{140}$, $Cys_{135}Cys_{139}Ala_{140}$, and $Ala_{135}Cys_{139}Cys_{140}$. The first three of these are simple amino acid replacements in the redox-active disulfide; the other two reposition the thiol pair by introducing a new cysteine into the active site at position 139. On the basis of examination of the glutathione reductase 1.9-Å crystal structure (Schulz et al., 1978), which serves as a model for mercuric reductase active

† Supported in part by NIH Grant 21643. K.G.A. was the recipient of a National Science Foundation Predoctoral Fellowship.

* To whom correspondence should be addressed.

‡ Present address: Department of Biochemistry, Duke Medical Center, Durham, NC 27710.

0006-2960/89/0428-1168$01.50/0

site geometry (11/14 residue identity), we anticipated that the two thiols in each of these latter mutants would remain in a dithiol oxidation state. Such mutants should hence retain the two-thiol inventory of the active site while eliminating the redox-active disulfide. A complete list of the active site mutants we have studied is shown in Table I. By examining the properties of the five new mutants as well as those of the original two serine mutants, we have gained considerable insight into how mercuric reductase functions.

Materials and Methods

Materials

Plasmid pJOE114 (Brown et al., 1983) was a generous gift of Dr. Nigel Brown of the Department of Biochemistry, University of Bristol, Bristol BS8 1TD, U.K. *Escherichia coli* strain W3110 lacI^q and the plasmid pSE181 were generously provided by Dr. Graham Walker of the Department of Biology, Massachusetts Institute of Technology, Cambridge, MA 02139. *E. coli* RZ1032 was a generous gift from Dr. Thomas Kunkel, Laboratory of Genetics, National Institute of Environmental Health Sciences, Research Triangle Park, NC 27709. *E. coli* strain JM101 and M13mp9 RF DNA and M13mp8 RF DNA were obtained from New England Biolabs. Plasmid pKK223-3 was obtained from Pharmacia.

All restriction enzymes, T4 polynucleotide kinase, T4 ligase, DNA polymerase I (Klenow fragment), and *Hind*III linkers were obtained from New England Biolabs. Calf intestinal phosphatase was obtained from Boehringer-Mannheim. Deoxyadenosine 5′-[α-^{35}S]-α-thiotriphosphate (>600 Ci/mmol) and adenosine 5′-[γ-^{32}P]triphosphate (>5000 Ci/mmol) were obtained from Amersham. $^{203}HgCl_2$ (1–20 Ci/g) was obtained from New England Nuclear.

SepPac columns were obtained from Waters, and Elutip-d columns were from Schleicher & Schuell. Orange A Matrex gel was purchased from Amicon Corp. P6-DG desalting resin and the TSK-250 HPLC gel filtration column were obtained from Bio-Rad.

$Hg(CN)_2$ was obtained from Aldrich. Thionicotinamide adenine dinucleotide phosphate was purchased from Sigma Chemical Co. Carba-1-deazariboflavin and 8-hydroxyriboflavin were generously provided by Merck, Sharp and Dohme Research Laboratories, Rahway, NJ.

Methods

Spectrophotometry. UV/vis spectra were recorded with a Perkin-Elmer 554, a Lambda 5, or a Hewlett-Packard 8452A spectrophotometer.

Oligonucleotide Synthesis. Oligonucleotides were synthesized by the solid-phase phosphotriester method using a Biosearch SAM ONE DNA synthesizer. Oligonucleotides were purified by reverse-phase SepPac chromatography followed by polyacrylamide gel electrophoresis. After electrophoresis the desired oligonucleotides were excised from the gel, eluted, concentrated, and desalted by using a Sephadex G-50 column. The oligonucleotides were then phosphorylated with 5′-[γ-^{32}P]ATP or unlabeled ATP by use of T4 polynucleotide kinase for use in mutagenesis.

DNA Methods. The procedures below apply to all cases except where noted in the text. All restriction digests and cohesive end ligations were carried out according to the conditions specified by the manufacturers. Blunt end ligation mixtures were supplemented with PEG to a final concentration of 12%. Filling in of 5′ overhangs, plasmid preparation, vector dephosphorylation, linker kinase treatment, and linker ligation were performed as described by Maniatis et al. (1982). Transformations were done by using $CaCl_2$ according to standard procedures (Maniatis et al., 1982), and phage were isolated according to the method of Zoller and Smith (1983). All restriction fragments and linearized vectors were isolated from agarose gels either by phenol extraction of low-melting agarose or by electrodialysis followed by purification on Elutip-d columns.

Mutagenesis. Oligonucleotide-directed mutagenesis was carried out by the method of Zoller and Smith (1983) with the exception of extending the mutagenesis primer in the presence of a universal primer (Zoller & Smith, 1984), located 280 bases from the Cys_{135} codon, and with deletion of the alkaline sucrose gradient centrifugation. An additional modification in which the template ssDNA was isolated from phage grown in a *ung*$^-$ strain (Kunkel, 1984) was used for two mutants, $Ala_{135}Cys_{139}Cys_{140}$ and $Ala_{135}Ala_{140}$. Primer specificity was evaluated by in vitro priming of standard Sanger sequencing reactions (Sanger et al., 1981). Optimal specificity was obtained by annealing 30 pmol of primer for the $Ala_{135}Cys_{140}$, $Cys_{135}Ala_{140}$, and $Cys_{135}Cys_{139}Ala_{140}$ mutants, 20 pmol of primer for the $Ala_{135}Ala_{140}$ mutant, and 10 pmol of primer for the $Ala_{135}Cys_{139}Cys_{140}$ to 1 pmol of template at 55 °C for 2 h. The $Ala_{135}Cys_{140}$ and $Cys_{135}Ala_{140}$ mutants were made by using M13ps1 (Schulz et al., 1985); the $Cys_{139}Ala_{140}$ mutant was made from M13ps5, and the $Ala_{135}Ala_{140}$ and $Ala_{135}Cys_{139}$ were made from M13ka1 (see below). For the mutagenesis reactions, extension and ligation were carried out for 18 h at 14 °C followed by transformation and phage isolation. The $Ala_{135}Cys_{140}$, $Cys_{135}Ala_{140}$, and $Cys_{135}Cys_{139}Ala_{140}$ mutants were screened by dot–blot hybridization with wash temperatures of 52 °C for the $Ala_{135}Cys_{140}$ primer (5′-GACATTGACGGCGGTGCC-3′; T_m = 60 °C), 54 °C for the $Cys_{135}Ala_{140}$ mutant (5′-GACGGCACAGCGCCGACAT-3′; T_m = 64 °C), and 53 °C for the $Cys_{135}Cys_{139}Ala_{140}$ mutant (5′-CACAGCGCAGA-CATTGAC-3′; T_m = 54 °C). Clones deemed positive by hybridization screening were retransformed, plaques were purified and rescreened by hybridization, and finally the presence of the desired mutation was confirmed by Sanger sequencing. The $Ala_{135}Ala_{140}$ (primer, 5′-GCACGGCA-CAGCGCCGACATT-3′; T_m = 62 °C) and $Ala_{135}Cys_{139}Cys_{140}$ (primer, 5′-GCACACAGCAGACATTG-3′; T_m = 52 °C) mutants were screened by single-lane Sanger sequencing followed by four-lane sequencing of clones which showed the appearance of a new band in the single-lane sequencing reactions. The resulting mutant plasmids are M13ps4 ($Ala_{135}Cys_{140}$), M13ps5 ($Cys_{135}Ala_{140}$), M13md1 ($Cys_{135}Cys_{139}Ala_{140}$), M13md4 ($Ala_{135}Ala_{140}$), and M13md5 ($Ala_{135}Cys_{139}Cys_{140}$).

Plasmid Constructions. (*A*) *pKAM1, pKAM2, and pMDM1.* M13ps4, M13ps5, and M13md1 were each digested with *Hind*III and *Sal*I and the resulting 1748 base pair fragments separated, ligated with pJOE114 previously cut with *Hind*III and *Sal*I, and dephosphorylated. The ligation mixtures were then used to transform *E. coli* W3110 lacI^q, and DNA from ampicillin-resistant clones was isolated. The presence of the desired insert was confirmed by restriction analysis with *Sal*I, *Hind*III, and *Nar*I. The resulting plasmids are pKAM1 ($Ala_{135}Cys_{140}$), pKAM2 ($Cys_{135}Ala_{140}$), and pMDM1 ($Cys_{135}Cys_{139}Ala_{140}$).

(*B*) *pKAO1 and pKAO2.* Plasmids pKAM1 and pKAM2 were each digested with *Ava*I, and the resulting fragments were then treated with Klenow fragment to fill in the recessed 3′ termini. The blunt-ended fragments were then separated by agarose gel electrophoresis and the desired 2708 bp fragments

purified and digested with *Nar*I. The products of these digests were then separated on a second agarose gel, and the desired 2102 bp fragments were then ligated to dephosphorylated pSE181 vector that had been cut with *Cla*I and *Sma*I. These ligation mixtures were used to transform *E. coli* W3110 lacI^q. Ampicillin-resistant clones were obtained, and the presence of the desired inserts was confirmed by restriction analysis with *Sal*I and by SDS gel electrophoresis of the crude sonicate after induction with IPTG.[1] Insertion of the above fragments afforded plasmids pKAO1 ($Ala_{135}Cys_{140}$) and pKAO2 ($Cys_{135}Ala_{140}$).

(*C*) *pMDO1 and pMDO2.* Plasmids pJOE114 and pMDM1 were digested with *Nar*I and *Not*I, the ends made blunt with Klenow fragment, and *Hin*dIII linkers ligated on. The ligation mixture was then digested with *Hin*dIII, and the products were separated on an agarose gel. The purified 1972 bp fragments were ligated to pKK223-3, previously cut with *Hin*dIII and dephosphorylated. The resulting mixture was then used to transform *E. coli* W3110 lacI^q, and plasmid DNA from ampicillin-resistant clones was isolated. Presence of the desired insert in the correct orientation was confirmed by restriction analysis with *Hin*dIII, *Sal*I, and *Eco*RI. Overproduction of mercuric reductase by these cells was demonstrated by SDS gel electrophoresis of crude extract prepared by sonication of cells induced with IPTG. The overproduction plasmids pMDO1 and pMDO2 express the wild-type and $Cys_{135}Cys_{139}Ala_{140}$ proteins, respectively.

(*D*) *pMDO3 and pMDO4.* Plasmid DNA from pMDO1 was linearized with *Sma*I and partially digested with *Sal*I and the resulting mixture separated on an agarose gel. The band containing DNA that had only been cut once with *Sal*I was excised from the gel and purified for use as a vector. M13md4 and M13md5 DNA was cut with *Nar*I, and the ends were made blunt with Klenow fragment and then cut with *Sal*I. After the fragments were separated on an agarose gel, the 584 bp fragment containing the N-terminus of merA was purified and ligated with the vector described above and used to transform *E. coli* W3110 lacI^q. Plasmid DNA from ampicillin-resistant clones was isolated, and the presence of the desired insert was confirmed by restriction analysis with *Hin*dIII, *Sal*I, and *Eco*RI. Production of mercuric reductase protein was demonstrated as described above for pMDO1. The resulting plasmids, pMDO3 and pMDO4, contain the $Ala_{135}Ala_{140}$ and $Ala_{135}Cys_{139}Cys_{140}$ mutations, respectively.

Mutant Sequencing. To verify that no undesired mutations had been introduced in the DNA during mutagenesis, *Nar*I/*Sal*I and *Nar*I/*Eco*RI fragments from the plasmids pKAM1, pKAM2, and pMDM1 were cloned into M13mp9 cleaved with *Nar*I and *Sal*I and M13mp8 cleaved with *Eco*RI and *Acc*I, respectively. These plasmids were then sequenced according to the Sanger method; regions containing sequences difficult to interpret were resequenced according to the deoxyinosine method of Mills and Kramer (1979) for additional verification. *Nar*I/*Eco*RI fragments from pMDO3 and pMDO4 cloned into M13mp8 were also similarly sequenced. The above sequencing allowed the entire *mer*A segments of DNA present in M13 during mutagenesis to be examined for any spurious mutations. The M13mp9 derivative containing the *Nar*I/*Sal*I fragment from pKAM1 is called M13ka1 and was used as a mutagenesis template as described above.

Enzyme Purification. The following procedure applies to the purification of the wild-type and all mutant enzymes. Throughout the procedure, transhydrogenase activity was used to follow the purification; the assay is described below. Cells (*E. coli* W3110 lacI^q/pPSO1, pPSO2, pPSO3, pKAO1, pKAO2, pMDO1, pMDO2, pMDO3, or pMDO4) were grown, induced, and harvested, and the protein was isolated as previously described (Schultz et al., 1985) except that TPCK, TLCK, and leupeptin were omitted from the lysis buffer.

Enzyme Assays. Hg(II)-, thio-$NADP^+$-, and DTNB-dependent NADPH oxidations were monitored at 37, 25, and 25 °C, respectively, in 80 mM sodium phosphate, pH 7.4, and 200 μM NADPH. Hg(II)- and thio-$NADP^+$-dependent NADPH oxidations were monitored at 340 nm (absorbance) or 470 nm (fluorescence). NADPH-dependent DTNB reduction was monitored at 440 nm (ϵ = 9.5 mM^{-1} cm^{-1}). Hg(II) reductase activity was monitored in the presence of 100 μM $HgCl_2$ and either 1 mM 2-mercaptoethanol or 0.5 mM EDTA. The high stability constants of Hg(II)–EDTA and $Hg(SR)_2$ ensure that all the Hg(II) is present in the chelated form. Transhydrogenase activity was monitored in the presence of 1 mM 2-mercaptoethanol and 100 μM thio-$NADP^+$ during enzyme purifications. For K_m and V_{max} determinations, enzyme samples were exhaustively dialyzed against 20 mM sodium phosphate and 0.5 mM EDTA, pH 7.4, to remove $NADP^+$ introduced during Orange A chromatography. DTNB reductase activity was monitored in the presence of 1 mM DTNB. One unit of enzyme activity is defined as the amount of enzyme that catalyzes the Hg(II)- or thio-$NADP^+$-dependent oxidation of 1 μmol of NADPH/min or the reduction of 0.5 μmol of DTNB/min.

Oxygen consumption assays were performed at 37 °C with a Yellow Springs Instrument Co. Model 53 biological oxygen monitor with air-saturated buffer and 150 μM NADPH. $Hg(CN)_2$-dependent stimulation of O_2 consumption was monitored in the presence of 100 μM $Hg(CN)_2$. Enzyme samples were dialyzed as described above. Production of H_2O_2 was confirmed by the addition of catalase to the reaction mixture after O_2 consumption began to level off.

Protein Concentration. Protein concentrations were determined by the method of Lowry (1951) with bovine serum albumin as a standard. Routine determination of enzyme concentration was based on flavin content, using an extinction coefficient determined by methods previously described (Schultz et al., 1985).

Molecular Mass Determination. Subunit molecular mass was estimated by SDS–polyacrylamide gel electrophoresis as described by Laemmli (1970). Native molecular masses were determined by HPLC gel filtration chromatography using a TSK-250 column (Bio-Rad) employing the conditions specified by the manufacturers.

Thiol Titrations. Thiols were titrated spectrophotometrically with DTNB as described previously (Fox & Walsh, 1982).

Anaerobic and Redox Titrations. Anaerobic and redox titrations were performed as previously described (Fox & Walsh, 1982) or by an enzymatic reduction method employing xanthine and xanthine oxidase (Massey et al., unpublished results).[2] To avoid formation of charge-transfer complexes

[1] Abbreviations: IPTG, ispropyl β-D-thiogalactopyranoside; DTNB, 5,5′-dithiobis(2-nitrobenzoate); TNB, 5-thio-2-nitrobenzoate; DTT, dithiothreitol; E_{ox}, oxidized form of wild-type mercuric reductase; EH_2, wild-type enzyme reduced with two electrons per monomer; EH_4, wild-type enzyme reduced with four electrons per monomer; EHR, two-electron-reduced wild-type enzyme treated with iodoacetamide; E-FAD, oxidized form of mutant enzymes; E-$FADH_2$, mutant enzymes reduced with two electrons per monomer; FAD, flavin adenine dinucleotide; $FADH_2$, dihydroflavin adenine dinucleotide; FMN, flavin mononucleotide; bp, base pairs of DNA.

with nicotinamides when undesired, $NADP^+$ was removed from all preparations by dialysis against 2 M KBr as previously described. The redox indicator dyes 1-deazariboflavin [$E^{\circ\prime}$ = −280 mV (Walsh et al., 1978)], 8-hydroxyriboflavin [$E^{\circ\prime}$ = −340 mV (Light & Walsh, 1980)], methylviologen [$E^{\circ\prime}$ = −449 mV (Wilson, 1978)], and benzylviologen [$E^{\circ\prime}$ = −358 mV (Wilson, 1978)] were used to determine oxidation–reduction potentials of the mutant mercuric reductases.

E-FADH$_2$/Mercury(II) Reoxidation Experiments. All reoxidation experiments were performed in anaerobic cuvettes equipped with two side arms and syringe fittings as previously described (Williams et al., 1979). All solutions were degassed by evacuating to 0.5 mmHg gas pressure after the sample had been cooled to −78 °C and maintaining the vacuum for 30 min followed by thawing and refreezing under Ar atmosphere; in all cases this was repeated at least three times. Enzyme samples were degassed at room temperature by treating them for 5 min under vacuum, followed by 1 atm of Ar for 30 s for a total of 10 cycles. The samples were stored and loaded into the anaerobic cuvettes under a He atmosphere in a glovebox. The mutant enzymes were then titrated with sodium dithionite until the enzyme was approximately 80% reduced. The reduced enzyme was allowed to equilibrate for 1 h at 37 °C and then monitored for an additional 30 min at the E_{ox} absorbance maximum to obtain a stable base line and verify that no leakage from atmospheric oxygen was occurring. Reoxidation of the reduced enzyme was initiated by tipping the desired mercury compound into the cuvette from a side arm and was monitored spectrophotometrically for at least 10 half-lives. Kinetic data were analyzed by a linear least-squares regression plot. Hg(II)–EDTA experiments contained 100 mM sodium phosphate, pH 7.5, 180 μM $HgCl_2$, 450 μM EDTA, and approximately 15 μM enzyme. Experiments with Hg(II)$(Cys)_2$ were identical except that they were supplemented to a final concentration of 1.8 mM cysteine. Reoxidation experiments with the model compounds FAD, FMN, riboflavin, 5-deazariboflavin, and 5-deaza-FAD were performed identically.

^{203}Hg(0) Volatility Assays. These assays are an anaerobic modification of the method previously described by Schottel (1978). All reactions were performed in 10-mL Wheaton vials fitted with double septa. Samples were degassed as described above in the E-$FADH_2$ reoxidation experiments. Reactions were initiated by adding NADPH and Hg(II)–EDTA via gas-tight syringes and carried out at 37 °C in a water bath. Aliquots (250 μL) were withdrawn at selected time intervals, and any Hg(0) produced was volatilized at 37 °C under a stream of Ar gas. Scintillation fluid (20 mL) was then added and the remaining radioactivity counted with a scintillation counter. Assay conditions were as follows: 100 mM sodium phosphate, pH 7.4, 91 μM $HgCl_2$, 230 μM EDTA, and 360 μM NADPH with approximately 2 μM enzyme in a total volume of 2.2 mL. Hg(II)$(Cys)_2$ experiments were identical except that cysteine was added to a final concentration of 260 μM.

FAD K_m Determinations. The apparent K_m for FAD was determined for the $Cys_{135}Cys_{139}Ala_{140}$ and $Ala_{135}Cys_{139}Cys_{140}$ mutants. For the determination of K_m, apoprotein was first prepared by dialysis of the holoprotein against 2 M KBr and 0.1 M sodium acetate, pH 4.5 at 4 °C. After desalting via a Sephadex G-25 column, the apoprotein was then reconstituted with FAD at various concentrations in 100 mM sodium phosphate, pH 7.4, at 4 °C for 2 h and the transhydrogenase activity determined. K_m was determined by a double-reciprocal plot of $1/v$ vs $1/[FAD]$ as described by Dixon and Kenworthy (1967).

Results and Discussion

Generation and Expression of Mutant Mercuric Reductases. The $Ala_{135}Cys_{140}$, $Cys_{135}Ala_{140}$, and $Cys_{135}Cys_{139}Ala_{140}$ mutants were generated by using the method of Zoller and Smith (1983) employing an M13 derivative containing a 1748 bp fragment from pJOE114. The two single Ala mutants required the use of primers resulting in double mismatches whereas the $Cys_{135}Cys_{139}Ala_{140}$ mutant possessed only a single mismatch when used with an M13 template containing the Ala_{140} mutation. Mutagenesis yields in the above cases were less than 0.3%, necessitating the screening of a large number of plaques. The $Ala_{135}Ala_{140}$ and $Ala_{135}Cys_{139}Cys_{140}$ double mutants were generated by using the Kunkel modification of the Zoller and Smith method (Kunkel, 1984); additionally, the insert size in the M13 template was reduced from 1748 to 584 bp. These improvements increased mutagenesis yields to 25% and 5% for the $Ala_{135}Ala_{140}$ and $Ala_{135}Cys_{139}Cys_{140}$ mutants, respectively.

After verification of the desired mutation by Sanger sequencing with the universal primer, the 1748 bp *Hin*dIII–*Sal*I fragments containing the $Ala_{135}Cys_{140}$, $Cys_{135}Ala_{140}$, and $Cys_{135}Cys_{139}Ala_{140}$ mutants were subcloned into pJOE114 to reconstruct the mutant merA genes. The resulting plasmids, pKAM1, pKAM2, and pMDM1, were then resequenced by directionally cloning fragments into M13mp8 and M13mp9 to confirm insertion of the mutant fragments and to verify that no additional mutations had been introduced during mutagenesis. The $Ala_{135}Ala_{140}$ and $Ala_{135}Cys_{139}Cys_{140}$ mutations were confirmed by sequencing the mutant M13 derivatives M13md4 and M13md5. Additionally, the mutant fragments were subcloned into M13mp8, which afforded clones in the opposite orientation thereby allowing the complete insert present in M13 during mutagenesis to be sequenced. The $Ala_{135}Ala_{140}$ and $Ala_{135}Cys_{139}Cys_{140}$ mutants were not subcloned into pJOE114 but were subcloned directly into the expression vector as discussed below.

To increase the production and facilitate purification of protein, all mutant mercuric reductase genes were placed in hybrid *tac* promoter plasmids. The $Ala_{135}Cys_{140}$ and $Cys_{135}Ala_{140}$ mutants were overexpressed by cloning the 2102 bp *Ava*I–*Nar*I fragments from pKAM1 and pKAM2 into the *Sma*I and *Cla*I sites of pSE181. Wild-type mercuric reductase and the $Cys_{135}Cys_{139}Ala_{140}$ mutant were overexpressed by cloning 1972 bp *Nar*I–*Not*I fragments from pJOE114 and pMDM1, respectively, into the *Hin*dIII site of pKK223-3 by using *Hin*dIII linkers, thus generating pMDO1 and pMDO2 containing the wild-type and $Cys_{135}Cys_{139}Ala_{140}$ mutant genes, respectively. pMDO1 was then conveniently used to construct the $Ala_{135}Ala_{140}$ and $Ala_{135}Cys_{139}Cys_{140}$ overproducers directly from the original M13 derivatives containing the mutations, thereby removing the need to subclone into pJOE114 prior to overproduction. Overexpression was simply accomplished

[2] The reduction potentials reported in this paper were determined by using the unpublished xanthine/xanthine oxidase method of Massey et al. The reduction potentials for the $Ser_{135}Cys_{140}$ and $Cys_{135}Ser_{140}$ mutant proteins have also been measured with sodium dithionite or light/EDTA as the electron source (Massey et al., unpublished results). These latter two methods are necessarily equilibrium methods since the concentrations of enzyme and dye species are calculated after all spectral changes have ceased. These methods give values that agree with those obtained from the xanthine/xanthine oxidase method within 3%. Similarly, the cooperativity effects observed in the xanthine/xanthine oxidase experiments are also seen in the sodium dithionite or light /EDTA titrations. After taking into account the close agreement between reduction potential values determined by different methods for the Cys to Ser mutants, we elected to use the xanthine/xanthine oxidase method due to its experimental simplicity.

Table II: Summary of Thiol Titration Data for Mutant Mercuric Reductases[a]

enzyme	-NADPH[b]	+NADPH[c]	+DTT
$Cys_{135}Cys_{140}$ (wild type)	2.2	4.3 (6.5)[d]	4.4[e]
$Ala_{135}Cys_{140}$	3.2	3.2	
$Cys_{135}Ala_{140}$	3.2	2.8	
$Ala_{135}Ala_{140}$	1.9	1.9	
$Cys_{135}Cys_{139}Ala_{140}$	3.9	3.9	
$Ala_{135}Cys_{139}Cys_{140}$	1.9	1.9	5.8

[a] Thiols reported as thiols per monomer. [b] All proteins were extensively dialyzed against 2 M KBr and hence possessed oxidized C-terminal thiols. See following paper (Miller et al., 1989). [c] Proteins were incubated on ice with NADPH for 1–2 min prior to denaturation. This short period of incubation appears insufficient for reduction of C-terminal thiols in wild-type enzyme. [d] After extended incubation with NADPH, reduction of C-terminal thiols is observed. See Miller et al. (1989). [e] The active site disulfide is reduced by DTT but reoxidizes under aerobic gel filtration conditions used to remove DTT prior to thiol titration. See Miller et al. (1989).

by subcloning the 584 bp *Nar*I–*Sal*I fragments from M13md4 and M13md5 into the *Sma*I and *Sal*I sites of pMDO1, thus generating pMDO3 and pMDO4 containing the $Ala_{135}Ala_{140}$ and $Ala_{135}Cys_{139}Cys_{140}$ mutations, respectively.

The resulting plasmids carrying the mutant mercuric reductases were expressed in *E. coli* W3110 lacI^q and induced with the gratuitous inducer IPTG. Mercuric reductase was present in crude extract as 5–10% of the total soluble protein based on the level of thio-NADP$^+$ transhydrogenase activity. The mutant enzymes were purified by the method of Schultz et al. (1985); the $Ala_{135}Cys_{140}$, $Cys_{135}Ala_{140}$, and $Ala_{135}Ala_{140}$ proteins were obtained in nearly quantitative yield while the $Cys_{135}Cys_{139}Ala_{140}$ and $Ala_{135}Cys_{139}Cys_{140}$ enzymes were obtained in lower yields of 38% and 20%, respectively, consistent with the slow loss of FAD described below. Although mutant enzymes appear more susceptible to proteolysis during purification, the addition of protease inhibitors to the lysis buffer had no protective effect.

Thiol Titrations. Enzyme thiol content was assessed in the absence (oxidized) and presence (reduced) of NADPH with DTNB as summarized in Table II. Enzymes were denatured with 5 M guanidine hydrochloride prior to titration. In the wild-type enzyme, the presence of two titratable thiols in the oxidized form and four titratable thiols upon reduction with NADPH is consistent with the existence of a redox-active disulfide (Fox & Walsh, 1983) and constitutes an appropriate standard with which the mutant enzymes can be compared. Both the $Ala_{135}Cys_{140}$ and $Cys_{135}Ala_{140}$ mutants contain, as anticipated, three titratable thiols per subunit in both the oxidized and reduced forms (3.2 and 3.2 for $Ala_{135}Cys_{140}$ and 3.2 and 2.8 for $Cys_{135}Ala_{140}$). The $Ala_{135}Ala_{140}$ mutant contains only two titratable thiols in both the oxidized and reduced forms (1.9 and 1.9 thiols). These results are consistent with the substitution of one cysteine by alanine in the single mutants and the substitution of two alanines for two cysteines in the double mutant and correspond to thiol count results observed with the single cysteine to serine mutants previously reported from this laboratory (Schultz et al., 1985).

In the case of the $Cys_{135}Cys_{139}Ala_{140}$ mutant, the presence of four titratable thiols per subunit in both the oxidized and reduced forms (3.9 thiols in both) is strong evidence that Cys_{135} and Cys_{139} are in a dithiol configuration and not in a disulfide. In contrast, only two thiols are titratable in the $Ala_{135}Cys_{139}Cys_{140}$ mutant in both the presence and absence of NADPH (1.9 and 1.9); however, pretreatment of this mutant with excess DTT followed by gel filtration results in protein in which a total of almost six thiols (5.8) can be titrated. These data demonstrate that in this mutant there are at least two disulfide bonds that are reducible by DTT but not by NADPH. Wild-type mercuric reductase has recently been shown to possess a second disulfide which is reducible upon incubation with DTT or NADPH [see following two papers in this issue (Moore & Walsh, 1989; Miller et al., 1989)], and it is likely that this disulfide (at the C-terminus) is one of those reduced after incubation of the $Ala_{135}Cys_{139}Cys_{140}$ mutant with DTT; the second reducible disulfide present in this mutant may be a disulfide between Cys_{139} and Cys_{140}.

Physical Properties. The mutant enzymes share many physical properties with the wild type. Both mutant and wild-type enzymes have dimeric structures as deduced from gel exclusion chromatography and have subunit molecular masses of 59 000 daltons and a proteolyzed form of 51 000 daltons as determined by SDS–polyacrylamide gel electrophoresis. The absorbance ratio A_{272}/A_{458} is 6.3 for the wild-type enzyme and varies from 6.3 to 6.8 for the $Ala_{135}Cys_{140}$, $Cys_{135}Ala_{140}$, and $Cys_{135}Cys_{139}Ala_{140}$ mutants. The A_{271}/A_{449} ratio for the $Ala_{135}Ala_{140}$ mutant is 5.7, which is low; this may be because a greater fraction of this enzyme exists in the proteolyzed "clipped" state as evidenced by SDS–polyacrylamide gel electrophoresis. The A_{274}/A_{450} ratio for the $Ala_{135}Cys_{139}Cys_{140}$ mutant protein as isolated is 9.3. This high value reflects the tendency of this protein to lose FAD upon high-salt dialysis and is seen quantitatively in the higher K_m for FAD for this mutant as noted below. It should also be pointed out that the $Ala_{135}Cys_{139}Cys_{140}$ protein appears more susceptible to proteolysis than other mutant mercuric reductases. Thus storage of this enzyme for more than 1–2 days at 4 °C results in extensive proteolysis, making many experiments difficult to perform.

All mutant proteins exhibit similar chromatographic behavior during purification on Orange A resin, reflecting the conservation of the NADPH binding domain thought to be essential in dye affinity chromatography. Except where noted below, all mutant enzymes also bind FAD with high affinity as evidenced by the retention of FAD by apoprotein even during exhaustive high-salt dialysis. After extensive dialysis against purification buffer subsequent to purification, NADP$^+$ remains bound to all mutants, giving rise to a variety of charge-transfer complexes and spectrally perturbed flavins. These complexes dissociate upon dialysis of the enzymes against 2 M KBr.

FAD K_m Determination. During the high-salt dialysis designed to remove enzyme-bound nicotinamide, we noted that the $Cys_{135}Cys_{139}Ala_{140}$ and $Ala_{135}Cys_{139}Cys_{140}$ mutants had lost a substantial portion of their bound FAD. This is in contrast to the remainder of the mutants as well as to the wild-type enzyme where flavin loss does not occur. The apparent K_m values for FAD were determined for these two mutants and the wild-type enzyme; the values are 290 nM, 890 nM, and 65 nM for the $Cys_{135}Cys_{139}Ala_{140}$, $Ala_{135}Cys_{139}Cys_{140}$, and wild-type proteins, respectively. Thus, the introduction of a cysteine at position 139 and the likely involvement of this residue in a disulfide with Cys_{140} substantially decrease the mutant apoenzyme's affinity for the FAD cofactor. For the $Cys_{135}Cys_{139}Ala_{140}$ mutant, the increased FAD K_m is likely to be due to the increased steric bulk of a cysteine versus a glycine, resulting in disruption of the FAD binding pocket; we note that the glycine preceding the distal cysteine (Cys_{140} in mercuric reductase) is absolutely conserved in all members of the disulfide oxidoreductase flavoprotein family (Williams et al., 1982), suggesting inflexibility due to steric bulk at that position. The higher FAD K_m value for the $Ala_{135}Cys_{139}Cys_{140}$ mutant indicates that additional

Table III: Spectroscopic Properties of Mutant Mercuric Reductases

enzyme	λ_{max} (nm)	ϵ at λ_{max} (mM^{-1} cm^{-1})	charge-transfer λ_{max} (nm)
$Cys_{135}Cys_{140}$ (wild-type E_{ox})[a]	458	11.3	none
$Cys_{135}Cys_{140}$ (wild-type EH_2)[a]	440	81	540
carboxymethyl-$Cys_{135}Cys_{140}$ (EHR)[a]	440	81	580
$Ala_{135}Cys_{140}$	435	8.6	560
$Ser_{135}Cys_{140}$[b]	440	9.5	500–540 (br)
$Cys_{135}Ala_{140}$	450	11.9	none
$Cys_{135}Ser_{140}$[b]	440	11.3	none
$Ala_{135}Ala_{140}$	449	11.5	none
$Cys_{135}Cys_{139}Ala_{140}$	449	12.8	none
$Ala_{135}Cys_{139}Cys_{140}$	449	11.6	622[c]

[a] Previously reported in Fox and Walsh (1983). [b] Previously reported in Schultz et al. (1985). [c] Charge-transfer absorbance of enzyme isolated by affinity chromatography in the presence of NADP(H).

factors are contributing to disruption of FAD binding; one explanation for this may lie in the geometrical constraints for having a CysCys peptide in a disulfide bond. As evidenced for both the crystal structure and theoretical calculations of the conformations of the L-CysCys dipeptide, it is found that the peptide bond (ω angle) must be in a cis configuration to enable disulfide bond formation (Caspasso et al., 1977). In wild-type mercuric reductase the Gly_{139}–Cys_{140} peptide bond is likely to be in a trans configuration (in glutathione reductase this bond is trans); however, in the $Ala_{135}Cys_{139}Cys_{140}$ mutant this bond may adopt a cis conformation to allow disulfide bond formation. A change of peptide bond conformation from trans to cis is likely to have a substantial effect on the protein structure and thereby on FAD binding.

Spectroscopic Properties. Wild-type mercuric reductase can exist in an oxidized state (E), a two-electron-reduced state (EH_2), and a four-electron-reduced state (EH_4), each of which have distinctive electronic absorbance spectra (Figure 1 and Table III). The oxidized state is characterized by a λ_{max} in the visible region at 458 nm (Fox & Walsh, 1982). EH_2 contains oxidized flavin and reduced disulfide (Cys_{135} and Cys_{140}) at the active site. This change is reflected in a 28% decrease in the 458-nm absorbance in the $NADP^+$-free enzyme, a shift in λ_{max} to 440 nm, and a new absorbance band at 540 nm (Figure 1A). This long-wavelength absorbance is ascribed to a charge-transfer complex between a thiolate anion (Cys_{140}) in the mercuric reductase active site and oxidized flavin (Fox & Walsh, 1982; Schultz et al., 1985). Further addition of reducing equivalents results in the loss of absorbance in both the long-wavelength absorbing chromophore (540 nm) and the flavin (440 nm) consistent with net four-electron reduction of the disulfide and the flavin (EH_4). The $Ala_{135}Cys_{140}$, $Cys_{135}Ala_{140}$, and $Ala_{135}Ala_{140}$ mutant enzymes all lack the redox-active disulfide and consequently have only a two electron equivalent capacity; the oxidized form of these mutants is denoted E while the two-electron-reduced form is denoted E-$FADH_2$.

(A) $Ala_{135}Cys_{140}$ Protein. The spectrum of the oxidized $Ala_{135}Cys_{140}$ enzyme (Figure 1B), with a λ_{max} at 435 nm (ϵ = 8.57 mM^{-1} cm^{-1}) and broad long-wavelength absorption at 560 nm, resembles that of EH_2 in the wild-type enzyme (Figure 1A) and imparts a green color to this enzyme as isolated. The presence of the 560-nm band in this mutant clearly demonstrates the involvement of Cys_{140} in the thiolate–flavin charge-transfer complex and is consistent with previously reported observations with the $Ser_{135}Cys_{140}$ mutant (Schultz et al., 1985). While the charge-transfer absorbance occurs in all spectra of mutants possessing a Cys_{140} thiol group, as well as in the spectra of the wild-type EH_2 (Fox & Walsh, 1982) and EHR (Fox & Walsh, 1983) enzymes (EHR is obtained by iodoacetamide alkylation of EH_2 and is predominantly composed of carboxymethylated Cys_{135}), the λ_{max} of the long-wavelength absorbance is different in each case (see Table III). Thus, the residue at position 135 clearly plays a role in modulating the energy of the charge-transfer absorbance. One explanation for this increasing charge-transfer energy in the progression from position 135 = carboxymethyl-Cys (λ_{max} = 580 nm), position 135 = Ala (λ_{max} = 560 nm), and position 135 = Cys (λ_{max} = 540 nm) to position 135 = Ser (λ_{max} = 500–540 nm) may be the increased capability of the more polar side chains to interact with the Cys_{140} thiolate anion. It is possible for the Ser_{135} hydroxyl to hydrogen bond to the thiolate of Cys_{140}; such an interaction would be considerably less favorable for a weak hydrogen bond donor such as the Cys_{135} SH. While Ala_{135} or carboxymethyl-Cys_{135} cannot interact with Cys_{140} in a direct manner, it is still possible that they could influence the environment of Cys_{140} by inductive means. All these different interactions with Cys_{140} are significant in defining the thiolate–flavin charge-transfer energy because the energy of this transition is dependent on the ionization potential of the thiolate anion (Stewart & Massey, 1985). Removing electron density from the sulfur atom by hydrogen bonding will result in an increased ionization energy, which will in turn cause a shift in the charge-transfer absorbance to shorter wavelengths. For mercuric reductase mutants, this is precisely what is observed. In elegant work performed on Old Yellow Enzyme, Massey and co-workers have demonstrated that the energy of charge-transfer complexation can be modulated by variation in the ionization energy of substrate donor ligands (Abramovitz & Massey, 1976) or by reconstitution of apoprotein with flavin analogues of varying electron affinity (Stewart & Massey, 1985). In this paper we demonstrate that the charge-transfer energy can also be tuned by site-directed mutagenesis directed at the environment of the electron donor.

(B) pK_a of Cys_{140}. The spectral properties of the $Ala_{135}Cys_{140}$ mutant also enable us to determine the pK_a of the thiolate anion involved in the charge-transfer complex by monitoring the 560-nm absorbance as a function of pH. As the pH is lowered, the spectrum approaches that of free FAD. These absorbance changes are compatible with protonation of the anionic electron donor (Cys_{140}) with consequent loss of the charge-transfer band. The titration curve is reversible down to pH 5 and affords a pK_a value of 6.3. This value is higher than that observed for the $Ser_{135}Cys_{140}$ mutant, pK_a = 5.2 (Schultz et al., 1985), and for wild-type EH_2, pK_a = 5.1 (Miller et al., unpublished results), and again demonstrates the importance of residue 135 in modulating the chemical behavior of Cys_{140}. For comparison, the pK_a of the corresponding cysteine in pig heart lipoamide dehydrogenase is less than 5.2 (Matthews & Williams, 1976) and that for yeast glutathione reductase is 4.8 (Arscott et al., 1981).

(C) Binding of Hg(II) to Cys_{140}. The charge-transfer absorbance has also been used to monitor the binding of Hg(II) to Cys_{140} by observing the mercury-dependent quenching of this long-wavelength spectral feature as shown in Figure 2. While the charge-transfer absorbance of the $Ala_{135}Cys_{140}$ protein can be quenched with as little as 3 equiv of $HgCl_2$ or $Hg(CN)_2$, the charge-transfer absorption completely returns upon addition of only 2 equiv of exogenous thiols. These results are in contrast to those performed on wild-type EH_2 where the charge-transfer absorbance remained largely quenched even after the addition of 10 equiv of external thiols (Miller et al., 1986). This weaker binding of Hg(II) by the

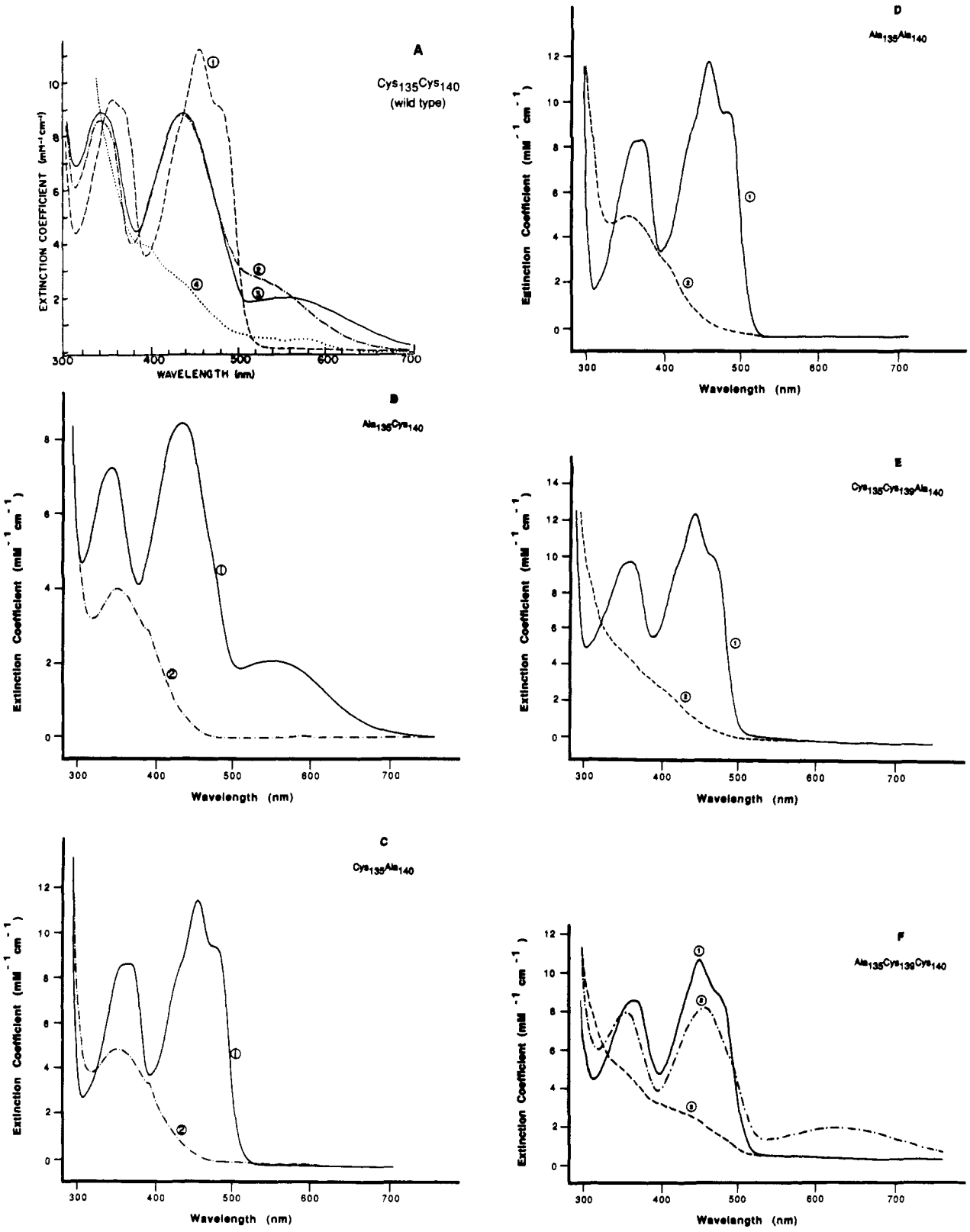

FIGURE 1: Optical spectra of oxidized and reduced forms of wild-type and mutant mercuric reductases. Except where noted below, all spectra were obtained from enzyme treated by high-salt dialysis to remove $NADP^+$. In (A), spectrum 1 is oxidized enzyme, spectrum 2 is two-electron-reduced enzyme, spectrum 3 is the iodoacetamide-treated two-electron-reduced enzyme, and spectrum 4 is four-electron-reduced enzyme. In (B–F), spectrum 1 is oxidized enzyme and spectrum 2 is two-electron-reduced enzyme. In (F), spectrum 3 is enzyme obtained directly from Orange A chromatography without high-salt dialysis. (A) Wild-type ($Cys_{135}Cys_{140}$) enzyme. (B) $Ala_{135}Cys_{140}$ enzyme. (C) $Cys_{135}Ala_{140}$ enzyme. (D) $Ala_{135}Ala_{140}$ enzyme. (E) $Cys_{135}Cys_{139}Ala_{140}$ enzyme. (F) $Ala_{135}Cys_{139}Cys_{140}$ enzyme.

$Ala_{135}Cys_{140}$ protein as compared to the wild-type EH_2 enzyme implicates Cys_{135} as a residue involved in mercury binding.

(D) $Cys_{135}Ala_{140}$ and $Ala_{135}Ala_{140}$ Proteins. The electronic absorption spectra of the oxidized $Cys_{135}Ala_{140}$ (Figure 1C) and $Ala_{135}Ala_{140}$ (Figure 1D) mutant mercuric reductases have λ_{max} at 450 nm (ϵ = 11.9 mM^{-1} cm^{-1}) and 449 nm (ϵ = 11.5 mM^{-1} cm^{-1}), respectively. These spectra resemble those of oxidized wild-type enzyme (Figure 1A) and the $Cys_{135}Ser_{140}$ mutant. However, the λ_{max} for each protein is shifted to a value between that of wild-type enzyme (458 nm) and that

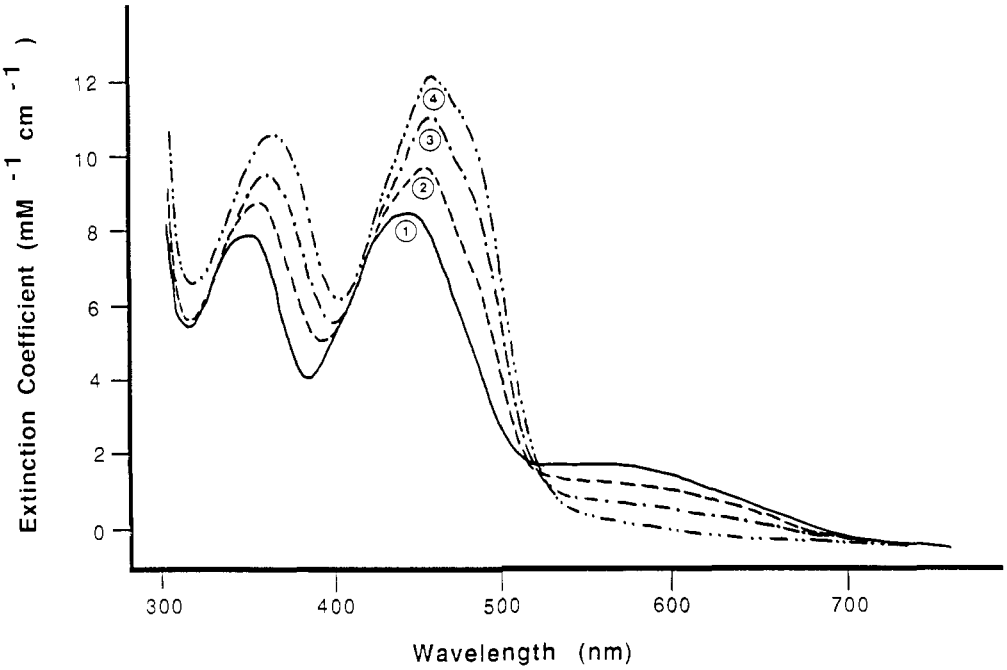

FIGURE 2: Titration of the $Ala_{135}Cys_{140}$ protein with $HgCl_2$. Spectrum 1 is enzyme obtained from high-salt dialysis (72 μM enzyme). Spectra 2, 3, and 4 are after the addition of $HgCl_2$ to a final concentration 94, 124, and 204 μM, respectively.

of the $Cys_{135}Ser_{140}$ mutant (440 nm). These differences may reflect either slight structural perturbations or small changes in the polarity of the flavin environment whose π to π^* transitions are known to be sensitive to the dielectric of the microenviroment (Rivlin, 1975).

Titration of the $Ala_{135}Cys_{140}$, $Cys_{135}Ala_{140}$, and $Ala_{135}Ala_{140}$ mutant enzymes with dithionite requires only two electron equivalents to reach the reduced flavin state. These results clearly indicate the absence of a redox-active disulfide and unambiguously demonstrate the involvement of Cys_{135} and Cys_{140} in the redox-active disulfide. Recent evidence has demonstrated the existence of a second, slowly reducible C-terminal disulfide in wild-type mercuric reductase [see following papers (Moore & Walsh, 1989; Miller et al., 1989)]. The inability to titrate the C-terminal disulfide via $FADH_2$ species in the above mutants also implies that an intact redox-active disulfide is essential for reduction of this second reducible disulfide.

(E) $Cys_{135}Cys_{139}Ala_{140}$ Protein. The spectrum of the oxidized $Cys_{135}Cys_{139}Ala_{140}$ mutant (Figure 1E) has a λ_{max} at 449 nm (ϵ = 12.8 mM^{-1} cm^{-1}) and closely resembles those of the $Cys_{135}Ala_{140}$ and $Ala_{135}Ala_{140}$ mutant enzymes (Figure 1C,D). No long-wavelength bands are present in the spectrum at pH 7.5, nor do any such bands appear when the enzyme is titrated up to pH 10, thus indicating the absence of thiolate–flavin charge-transfer interactions. This suggests that Cys_{139} is not able to engage in charge-transfer complexation either because it cannot interact at the necessary site on the isoalloxazine ring or because Cys_{139} is not positioned proximal to the flavin. This is in contrast to the prediction from the glutathione reductase crystal structure (Schultz et al., 1978) used as model in our mutagenesis studies. Titration of the oxidized $Cys_{135}Cys_{139}Ala_{140}$ enzyme with dithionite leads to loss of the 449-nm flavin band consistent with generation of E-$FADH_2$. A two-electron capacity per subunit also demonstrates that Cys_{135} and Cys_{139} do not form a redox-active disulfide.

(F) $Ala_{135}Cys_{139}Cys_{140}$ Protein. Upon initial isolation from an Orange A affinity column, the $Ala_{135}Cys_{139}Cys_{140}$ mutant mercuric reductase possesses a long-wavelength absorbance centered at 620 nm (see Figure 1F, curve 3). However, over a 5-day period this long-wavelength band decays to a featureless base line with a concurrent increase in extinction of the main flavin band (Figure 1F, curve 1). Addition of DTT to the 5-day-old sample resulted in regeneration of the long-wavelength absorbance along with reduction of extinction in the normal flavin band. These results are consistent with Cys_{140} forming a disulfide bond that is reducible with DTT. Initially, efforts to generate such a charge-transfer complex by DTT treatment of enzyme that had been dialyzed against high salt were unsuccessful. However, addition of $NADP^+$ to the enzyme treated with DTT restores the long-wavelength absorbance. This dramatic effect of $NADP^+$ on charge-transfer absorbance is similar to that previously observed with *E. coli* lipoamide dehydrogenase EH_2 (Wilkinson & Williams, 1979b). Titration of enzyme dialyzed against (Figure 3, curve 1) high salt, pretreated with DTT, with $NADP^+$ led to the appearance of a broad 622-nm-centered absorbance and ca. 15% bleaching of the flavin chromophore (Figure 3, curve 4) whereas titration without pretreatment with DTT resulted in only a slight loss of vibronic resolution in the main flavin band without appearance of the long-wavelength absorbance (Figure 3, curve 3). These complexes were stable under aerobic conditions over periods of at least several minutes; thus the involvement of any reduced flavin species is unlikely.

To verify that we were not observing an NADPH–FAD charge-transfer complex, a titration of the mutant enzyme (dialyzed against high salt) with NADPH was performed. Titration with NADPH under anaerobic conditions did lead to isosbestic formation of a long-wavelength absorbance of low extinction centered at 576 nm along with a decrease in the 450-nm flavin absorbance without loss of vibronic resolution. (Similar results are obtained in titrations with NADPH of the $Ala_{135}Ala_{140}$ mutant, which lacks both active site thiols, suggesting that a thiolate–flavin charge-transfer complex is not involved.) After the cuvette was opened to air, addition of DTT resulted in a shift of the long-wavelength absorbance to 620 nm. A similar titration with NADH [NADH is known to have a much higher K_m for wild-type mercuric reductase (Fox & Walsh, 1982) and thus does not form persistent charge-transfer complexes) led only to partial reduction of the

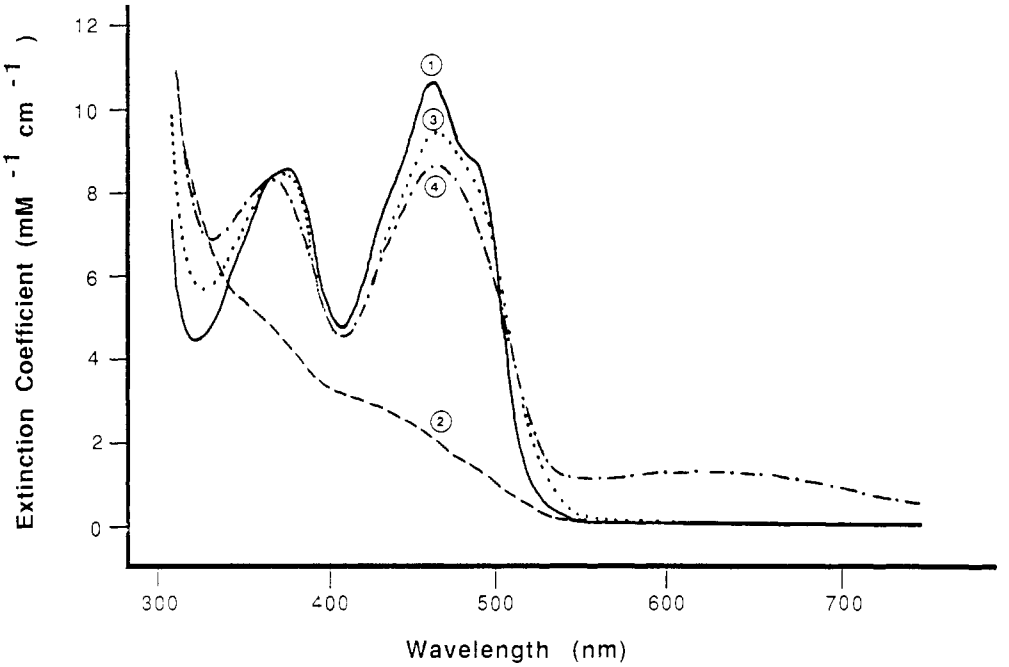

FIGURE 3: Charge-transfer absorbance of the $Ala_{135}Cys_{139}Cys_{140}$ protein can be generated from oxidized enzyme by the addition of $NADP^+$ and DTT. Spectrum 1 is the oxidized enzyme obtained from high-salt dialysis. Spectrum 2 was obtained by dithionite titration of oxidized enzyme. Spectrum 3 was obtained by incubation of oxidized enzyme with $NADP^+$ to a final concentration of 200 μM. Spectrum 4 was obtained by titrating oxidized enzyme previously reacted with 10 mM DTT with 200 μM $NADP^+$ at 4 °C.

flavin to $FADH_2$ with no development of long-wavelength absorbance. At the end of this titration, addition of DTT had no effect on the spectrum. We attribute the 576-nm complex observed in this NADPH titration to be a pyridine nucleotide complex with enzyme–FAD, distinct from the 622-nm complex which we believe to be due to a thiolate–flavin charge-transfer complex in the presence of $NADP^+$. Finally, titration of KBr-dialyzed mutant enzyme with sodium dithionite required only two electron equivalents to reach a reduced flavin species, thus demonstrating that, on a time scale of hours, the FAD moiety is the only group present in the enzyme reducible by dithionite. The relationships between various spectral forms of the $Ala_{135}Cys_{139}Cys_{140}$ mutant are shown schematically in Figure 4.

The above data strongly indicate that the $Ala_{135}Cys_{139}Cys_{140}$ mutant contains a disulfide which is reducible with DTT and that reduction of this disulfide is coupled with spectral changes similar to those observed in mercuric reductases possessing thiolate–flavin charge-transfer bands. Since Cys_{140} (the likely thiolate donor) is not involved in a disulfide bond in any other mutant mercuric reductases, we propose that, in the case of the $Ala_{135}Cys_{139}Cys_{140}$ mutant, Cys_{140} must exist in a disulfide with Cys_{139}, the new thiol introduced by mutagenesis. Such disulfides between adjacent Cys residues are rare in protein structures (Kao & Karlin, 1986) and, at least in model systems, are known to contain cis peptide bonds (Capasso et al., 1977). The optical properties of the $Ala_{135}Cys_{139}Cys_{140}$ mutant enzyme provide a facile way of examining the behavior of a Cys–Cys disulfide within a protein.

While the above-postulated disulfide is reducible with DTT, it does not appear to be reducible with dithionite, NADPH, or NADH, at least on the time scale of hours used in our titration experiments. Thus, this postulated active site disulfide remains locked in a conformation that is not well positioned for electron transfer from the $FADH_2$ moiety in contrast to the wild-type $Cys_{135}Cys_{140}$ disulfide.

Oxidation–Reduction Potentials.[2] The reduction potentials of the mutant enzymes were estimated by the enzymatic xanthine oxidase method as described by Massey et al. (unpublished results) in 80 mM sodium phosphate (pH 7.4) in the presence of the redox indicator dyes 1-deazariboflavin or benzylviologen for the $Cys_{135}Ala_{140}$, $Ala_{135}Ala_{140}$, and $Cys_{135}Cys_{139}Ala_{140}$ mutant enzymes and methylviologen or benzylviologen for the $Ala_{135}Cys_{140}$ mutant. Because of complications due to dissociation of FAD from the $Ala_{135}Cys_{139}Cys_{140}$ mutant, no redox titrations were performed on it. The midpoint potential in wild-type enzyme of the E/EH_2 couple is −269 mV, and it is −335 mV for the EH_2/EH_4 couple (Fox & Walsh, 1982). The latter value was calculated from the extent of disproportionation of EH_2 at equilibrium as described by Matthews and Williams (1976). For wild-type enzyme, the slope of a plot of E' vs log (E/EH_2) was 28 mV, which compared favorably with the theoretical value of 30 mV for a two-electron process [derived from the Nernst equation, $E' = E^{\circ\prime} + (RT/nF)$ log (ox/red); when $n = 2$, $RT/nF = 30$ mV]. In contrast, plots of E' vs log (E/EH_2)

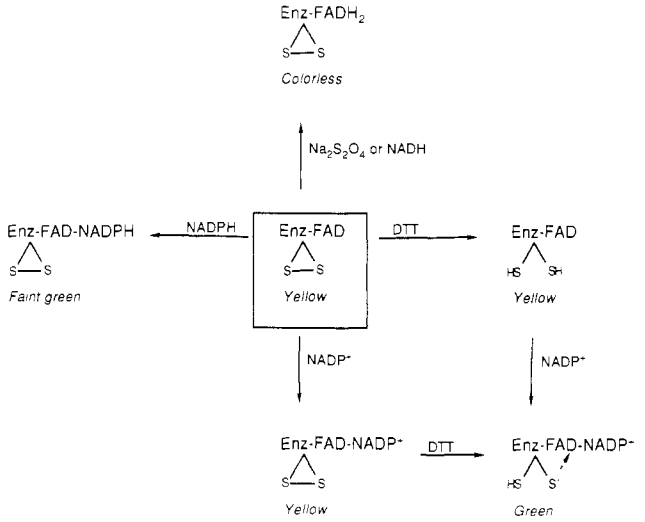

FIGURE 4: Spectrally distinct forms of the $Ala_{135}Cys_{139}Cys_{140}$ protein. The relationships between spectral forms of the $Ala_{135}Cys_{139}Cys_{140}$ protein and the enzyme obtained from high-salt dialysis (shown in the box) are shown.

Table IV: Mercury-Independent Catalytic Activities[a] and Reduction Potentials of Mercuric Reductases

enzyme	transhydrogenation k_{cat} (min^{-1})[b]	transhydrogenation K_m (μM)[b]	O_2 reduction TN (min^{-1})[c]	DTNB reduction TN (min^{-1})[c]	reduction potential $E^{\circ\prime}_1$ (mV)[d]	reduction potential $E^{\circ\prime}_2$ (mV)[d]
$Cys_{135}Cys_{140}$ (wild type)	54	0.80	2.0	20[e]	−269 (E_{ox}/EH_2), −335 (EH_2/EH_4)[f]	
$Ala_{135}Cys_{140}$	250	4.9	3.4	2.0	−321	−369
$Ser_{135}Cys_{140}$	6.0	3.0	0.2	none	−393	−428[g]
$Cys_{135}Ala_{140}$	330	4.0	7.2	1.0	−307	−351
$Cys_{135}Ser_{140}$	84	3.0	2.0	3.0	−326	−375[g]
$Ala_{135}Ala_{140}$	320	0.70	23	none	−291	−327
$Cys_{135}Cys_{139}Ala_{140}$	36	3.5	12	0.40	−290	−337
$Ala_{135}Cys_{139}Cys_{140}$	21[h]		56	none	−280 to −300[i]	

[a] Activities expressed as turnover numbers per monomer per minute. [b] In this case, k_{cat} is an apparent k_{cat} since only one substrate (NADPH) was varied. K_m is for NADPH. [c] TN is a turnover number determined under one set of conditions (i.e., neither substrate concentration was varied). [d] $E^{\circ\prime}_1$ and $E^{\circ\prime}_2$ refer to the first and second FAD redox potential per dimer as discussed under O_2 Reduction and Transhydrogenation. [e] A previous value of 440 min^{-1} (Schultz et al., 1985) was not reproducible. [f] Previously reported in Fox and Walsh (1982). No two-site analysis has been performed. Note that the EH_2/EH_4 value is the flavin redox potential for wild-type enzyme. [g] These values were determined by Massey and Miller (unpublished results). [h] Due to the instability of this protein no K_m has been determined. [i] Due to the tendency of this mutant protein to lose FAD it has not been possible to determine the FAD redox potential in lengthy redox titrations. The −280- to −300-mV range reported here is estimated by NADH titration.

[or, more conveniently, plots of log (E/EH_2) vs log (dye_{ox}/dye_{red})] for the mutant enzymes resulted in n values closer to 1 than to 2. Massey et al. (unpublished results) have suggested that determinations of these reduction potentials are complicated by the possibility that the flavins on the two subunits display cooperativity. Accordingly, when the data are replotted assuming that the two subunits contribute equally toward the absorbance spectra and that their reduction potentials are sufficiently different to allow the titration of at least 90% of the first subunit to be complete before the second subunit is titrated, slopes that give n values closer to 2 are obtained. Additional experiments are necessary to determine the cause of this cooperative behavior and are not reported here.

The data in Table IV show that the E-FAD/E-$FADH_2$ reduction potentials for mutant mercuric reductases vary over a 100-mV range and that the wild-type enzyme EH_2/EH_4 couple lies within this range. Examination of the data for the Cys to Ala mutant proteins reveals the dominant influence that the charge-transfer cysteine, Cys_{140}, exerts on the flavin reduction potential. Compared to the $Ala_{135}Ala_{140}$ mutant ($E^{\circ\prime}$ = −291 mV), the $Ala_{135}Cys_{140}$ protein ($E^{\circ\prime}$ = −321 mV) reduction potential has decreased 30 mV, reflecting a 1.4-kcal stabilization of the oxidized FAD cofactor attributable to charge-transfer complexation. Although the charge-transfer interaction dominates the FAD redox behavior, the residue at position 135 is clearly involved as well. This is demonstrated by the 16-mV decrease in reduction potential of the $Cys_{135}Ala_{140}$ protein ($E^{\circ\prime}$ = −307 mV) as compared to the $Ala_{135}Ala_{140}$ ($E^{\circ\prime}$ = −291 mV) protein. This decrease may be due to interaction of Cys_{135} with some portion of the FAD locus. Finally, the additivity of the effects due to individual residues seen with the Cys to Ala mutants is important. The 30-mV difference between $Ala_{135}Cys_{140}$ and $Ala_{135}Ala_{140}$ together with the 16-mV difference between $Cys_{135}Ala_{140}$ and $Ala_{135}Ala_{140}$ predict a value of −337 mV for the wild-type ($Cys_{135}Cys_{140}$) EH_2/EH_4 couple; the experimentally determined value is −335 mV.

In contrast to the predictable redox behavior of the Cys to Ala proteins, the redox properties of the Cys to Ser mutant proteins are complex. Comparison of the reduction potentials of the $Ala_{135}Cys_{140}$ and $Ser_{135}Cys_{140}$ mutant proteins reveals that the presence of the hydroxyl functionality at position 135 results in a decrease in reduction potential of 72 mV (3.3 kcal). While it is clear that the presence of this hydroxyl group at position 135 reduces the pK_a of Cys_{140} from 6.2 in the $Ala_{135}Cys_{140}$ protein to 5.2 (Schultz et al., 1985) in the $Ser_{135}Cys_{140}$ enzyme, it is unclear whether this perturbation of the Cys_{140} environment or some direct interaction between Ser_{140} and the FAD is responsible for the 72-mV decrease in reduction potential. A similar ambiguity exists for the $Cys_{135}Ser_{140}$ protein whose reduction potential is 19 mV less than that of $Cys_{135}Ala_{140}$. In this case the $Cys_{135}Ser_{140}$ protein's flavin redox properties may result from hydrogen bonding between the serine hydroxyl and flavin O-4 or N-5 acceptor sites.

The reduction potential of the $Cys_{135}Cys_{139}Ala_{140}$ mutant ($E^{\circ\prime}_1$ = −290 mV) is similar to that of the $Cys_{135}Ala_{140}$ protein, indicating that the Gly_{139} to Cys_{139} mutation has little effect on the FAD redox behavior. Due to the instability of the $Ala_{135}Cys_{139}Cys_{140}$ protein and its higher FAD K_m, we have not been able to determine its reduction potential in lengthy redox titrations; however, we estimate by titration with NADH that the value is in the range of −280 to −300 mV.

Aerobic Enzyme Assays. We have assayed six NADPH-dependent activities in both the wild-type and mutant mercuric reductases: transhydrogenation (thio-$NADP^+$/NADPH), O_2 reduction, aryl disulfide reduction, and $Hg(SR)_2$, $Hg(CN)_2$, and Hg(II)–EDTA reduction.

(A) O_2 Reduction and Transhydrogenation. Wild-type mercuric reductase as well as all mutant enzymes catalyze transhydrogenation reactions between pyridine nucleotides and reduce O_2 with the indicated stoichiometry:

$$\text{NADPH} + \text{thio-NADP}^+ \rightarrow \text{NADP}^+ + \text{thio-NADPH} \quad (1)$$

$$\text{NADPH} + O_2 + H^+ \rightarrow \text{NADP}^+ + H_2O_2 \quad (2)$$

Kinetic data for all active site mutants produced to date are shown in Table IV. Of the Cys to Ala mutants, the $Ala_{135}Cys_{140}$ protein has the lowest rates for transhydrogenation and O_2 reduction of 252 min^{-1} and 3.4 min^{-1}, respectively. The $Cys_{135}Ala_{140}$ and $Ala_{135}Ala_{140}$ enzymes have similar transhydrogenation k_{cat} values of 328 min^{-1} and 323 min^{-1}, respectively; however, these same proteins differ substantially in their O_2 reduction rates of 7.2 min^{-1} ($Cys_{135}Ala_{140}$) and 23 min^{-1} ($Ala_{135}Ala_{140}$), respectively. The double mutants, $Cys_{135}Cys_{139}Ala_{140}$ and $Ala_{135}Cys_{139}Cys_{140}$, have transhydrogenation k_{cat} values of 36 min^{-1} and 21 min^{-1}, respectively, which are greatly reduced relative to other mutant enzymes. In contrast, the O_2 reduction rates for these two mutant proteins, 12 min^{-1} for the $Cys_{135}Cys_{139}Ala_{140}$ protein and 56 min^{-1} for the $Ala_{135}Cys_{139}Cys_{140}$, are quite high. The large variations in enzymatic rates observed with the mutant proteins led us to search for a free energy relationship (Gernstein & Jencks, 1964) between reaction velocity and

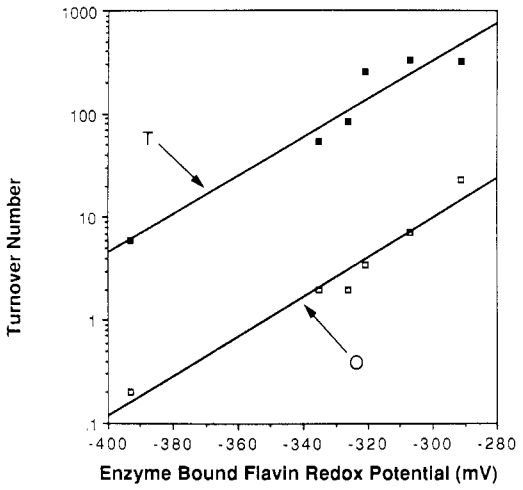

FIGURE 5: Correlation between transhydrogenation and O_2 reduction rates and enzyme-bound reduction potentials for wild-type and mutant mercuric reductases. Transhydrogenation k_{cat} values are represented by (■), and O_2 reduction rate values are given by (□). Line (T) indicates the best fit obtained from least-squares linear regression analysis of transhydrogenation data. Line (O) indicates a similar fit for O_2 reduction rates.

flavin reduction potential. To determine the extent of correlation, we have plotted the log (rate) values for both O_2 reduction (turnover number) and transhydrogenation (k_{cat}) vs reduction potential (Figure 5) for all mutant mercuric reductases except those mutants that introduce a Gly to Cys substitution at position 139; these mutants were not included since results discussed above clearly demonstrate the partial disruption of their FAD binding domains. For all mutant enzymes, the $E^{\circ\prime}_1$ (FAD → $FADH_2$) reduction potential value was used[3] while the EH_2/EH_4 (FAD → $FADH_2$) couple was used for the wild-type enzyme. The plots have a slope of 0.019 mV^{-1} for both O_2 reduction (correlation coefficient $r = 0.98$) and transhydrogenation ($r = 0.97$).

The above linear relationship is important because it implies that the variation in catalytic rate for specific reactions observed for the mutant enzymes is due principally to alterations in the FAD redox properties and not to random perturbations in enzyme structure. Additionally, it demonstrates that a chemical step involving flavin redox chemistry is at least partially rate determining. Both transhydrogenation and O_2 reduction require hydride transfer from NADPH to generate bound $FADH_2$; subsequently the two reaction pathways diverge. In transhydrogenation it is likely that a second hydride-transfer step, back from $FADH_2$ to thio-$NADP^+$, occurs, whereas in O_2 reduction FAD C-4a hydroperoxide formation followed by elimination of H_2O_2 takes place. We have examined the kinetics of the transhydrogenation activity for the mutant mercuric reductases using (4*S*)-[^{2}H]NADPH as a substrate (Fox & Walsh, 1982) to determine whether hydride transfer from dihydronicotinamide to FAD is rate limiting. No kinetic isotope effect on V_{max} was observed, suggesting that hydride transfer to flavin is not rate determining, consistent with similar stopped-flow experiments by Sahlman et al. (1986) performed on wild-type mercuric reductase. From their results, Sahlman et al. (1986) have proposed that the reactions of wild-type mercuric reductase with pyridine nucleotides are rate limited by $NADP^+$ release from the reduced enzyme. Thus, for the reactions of interest we can write $v = k_{eff}$[E-$FADH_2$–$NADP^+$], where v is the velocity of the reaction and k_{eff} is a net rate constant for $NADP^+$ dissociation (Cleland, 1975). The [E-$FADH_2$–$NADP^+$] is dependent on the position of the internal equilibrium reaction E-FAD–NADPH → E-$FADH_2$–$NADP^+$ which is directly related to the E-FAD/E-$FADH_2$ reduction potential. Variation of this reduction potential would then give rise to a linear relationship between log v and $E^{\circ\prime}$ as we have observed with mutant mercuric reductases. Further kinetic experiments are necessary to substantiate this hypothesis.

(*B*) *DTNB Reduction.* Wild-type mercuric reductase reduces the aryl disulfide DTNB ($v = 20$ min^{-1}) as well as the aliphatic disulfides dimethyl disulfide and cystine dimethyl diester (data not shown) according to the generalized equation, RSSR + NADPH + H^+ → 2RSH + $NADP^+$. As shown in Table IV, the $Cys_{135}Ser_{140}$, $Ala_{135}Cys_{140}$, $Cys_{135}Ala_{140}$, and $Cys_{135}Cys_{139}Ala_{140}$ mutant enzymes reduce DTNB at rates of 3 min^{-1}, 2 min^{-1}, 1 min^{-1}, and 0.4 min^{-1}, respectively, emphasizing the requirement for at least one active site thiol. The $Ser_{135}Cys_{140}$, $Ala_{135}Ala_{140}$, and $Ala_{135}Cys_{139}Cys_{140}$ mutant proteins show no detectable reduction of DTNB. Reduction of DTNB by wild-type mercuric reductase is thought to occur by a mechanism that parallels glutathione reductase (Pai & Schultz, 1983); however, in mutant mercuric reductases this mechanism is precluded by the absence of an intact redox-active disulfide. Instead, reduction may then occur slowly through direct reduction of an enzyme thiol/TNB mixed disulfide by $FADH_2$. The fact that enzyme-bound $FADH_2$ can transfer electrons to loci other than Cys_{140} demonstrates that, at least in the case of the mutant enzymes at rates up to 3 min^{-1}, all mercuric reductase redox chemistry need not be limited to that which can be carried out by a redox-active disulfide. The direct reduction of substrates by reduced flavin intermediates is an important generalization underlying the chemistry performed by all mutant mercuric reductases.

(*C*) *Aerobic Mercuric Reductase Assays.* The assay for mercuric ion reduction by mercuric reductase is measured by subtracting the background oxidase rate from the rate of NADPH consumption following Hg(II) addition. For the wild-type enzyme, addition of $Hg(SR)_2$ results in complete reduction of Hg(II) to Hg(0) whereas the addition of $Hg(CN)_2$ or Hg(II)–EDTA leads to partitioning of Hg(II) between reduction and inhibition. Full activity can be restored by the addition of thiols (Rinderle et al., 1983).

In the case of all mutant proteins except the $Ser_{135}Cys_{140}$ enzyme, addition of any Hg(II) compound results in a decrease in NADPH consumption, which for the $Cys_{135}Ser_{140}$ mutant enzyme was originally thought (Schultz et al., 1985) to be due to enzyme inactivation similar to that observed for the wild type with Hg(II)–EDTA. However, by examining the effect of Hg(II) salts on O_2 consumption rates as determined by using an O_2 electrode, it is clear that this apparent inactivation is due to an overall decrease in the O_2 consumption rate upon Hg(II) binding and not due to partitioning between Hg(II) turnover and inactivation as was previously reported. The mechanism via which Hg(II) addition results in suppression of the O_2 reduction activity remains unclear but could involve blockage of the approach of O_2 to $FADH_2$ or changes in flavin reduction potential.

Addition of $Hg(CN)_2$ to the $Ser_{135}Cys_{140}$ enzyme in the presence of NADPH results in an increase in NADPH consumption, initially ascribed to Hg(II) reduction (Schultz et

[3] We have used the $E^{\circ\prime}_1$ values since, in reduction of a dimer possessing two unequal sites, the site of higher reduction potential must be reduced first and hence must participate in catalysis. At present we have no evidence as to whether both active sites per dimer are catalytically active or not. If we use the average of $E^{\circ\prime}_1$ and $E^{\circ\prime}_2$ values for each mutant, we obtain a correlation of 0.017 mV^{-1} for transhydrogenation ($r = 0.90$) and 0.019 mV^{-1} for O_2 reduction ($r = 0.96$).

Table V: Pseudo-First-Order Enzyme–$FADH_2$[a] Reoxidation Kinetic Constants for Mutant Mercuric Reductases. Reoxidation by Hg(II)–EDTA

enzyme	Hg(II)–EDTA rate (min^{-1})	correlation coeff
$Ala_{135}Cys_{140}$	0.24	1.0
$Ser_{135}Cys_{140}$	0.79	0.99
$Cys_{135}Ala_{140}$	0.027	0.99
$Cys_{135}Ser_{140}$	0.059	0.99
$Ala_{135}Ala_{140}$	0.016	1.0
$Cys_{135}Cys_{139}Ala_{140}$	0.16	1.0
$Ala_{135}Cys_{139}Cys_{140}$	0.11	1.0
$Cys_{135}Cys_{140}$ (wild type)	>36[b]	
FAD	0.30	1.0

[a] Note that the reduced flavin form of wild-type enzyme is EH_4. [b] This value was estimated as described in the text and hence represents only a lower limit for the rate of reoxidation of native EH_4 by Hg(II)–EDTA.

al., 1985). However, we have now demonstrated in two types of experiments that this Hg(II)-dependent increase in NADPH consumption is due to a stimulation of the O_2 reduction rate and not to Hg(II) reduction. First, the O_2 reductase activity, as observed by O_2 electrode, increased 35-fold from 0.2 min^{-1} to 7 min^{-1} when 200 μM $Hg(CN)_2$ was added to the asssay solution. Second, no appreciable $Hg(CN)_2$-dependent oxidation of NADPH was observed under anaerobic conditions although consumption of NADPH was observed upon bubbling air into the assay mixture. It should be emphasized that the $Ser_{135}Cys_{140}$ mutant is the only mutant mercuric reductase whose O_2 reduction rate is stimulated by Hg(II) addition and that the origin of this anomaly is unknown.

Anaerobic Single-Turnover Assays of $Hg(SR)_2$ and Hg(II)–EDTA. Since all Hg(II) reduction assays of mutant mercuric reductases in aerobic solution gave ambiguous results due to the complicating effects of the O_2 reduction activity, we turned to anaerobic assays. To detect low levels of Hg(II) reduction, we used a highly sensitive assay that examined only a single turnover event. In this assay, mutant enzymes were first titrated to their reduced flavin state; a Hg(II) compound was then added and the rate of reoxidation of the E-$FADH_2$ species to E-FAD measured spectrophotometrically. Since these experiments were performed in the presence of excess Hg(II), a pseudo-first-order rate constant could be calculated and compared for different mutant enzymes. In addition to performing these assays on all mutant mercuric reductases, we have also examined the reoxidation of wild-type EH_4 as well as free $FADH_2$. For the wild-type enzyme, reoxidation was 95% complete in 5 s, allowing only a crude estimation of the reoxidation rate [$E(t) = E_0 \exp(-kt)$; hence ln 0.05 = $-k(5s)$, $k > 36$ min^{-1}]. Pseudo-first-order reoxidation rate constants and correlation coefficients are given in Table V. Given the excellent fit of the data in ln ($FADH_2$) vs time plots as evidenced by the range in correlation coefficients from 0.99 to 1.00, it is clear that all mutant enzymes reduce Hg(II) compounds in a reaction obeying pseudo-first-order kinetics. Examination of the rate data for Hg(II)–EDTA shows that the mutant E-$FADH_2$ enzymes are reoxidized at rates that vary over a 50-fold range and that the mutant with the fastest rate of reoxidation, $Ser_{135}Cys_{140}$, does so still at least 46 times slower than wild-type EH_4. The mutant enzymes, $Ser_{135}Cys_{140}$ (k_{reox} = 0.79 min^{-1}) and $Ala_{135}Cys_{140}$ (k_{reox} = 0.24 min^{-1}), which both retain Cys_{140}, are reoxidized much more rapidly than the $Cys_{135}Ser_{140}$ (k_{reox} = 0.059 min^{-1}), $Cys_{135}Ala_{140}$ (k_{reox} = 0.027 min^{-1}), and $Ala_{135}Ala_{140}$ (k_{reox} = 0.016 min^{-1}) proteins which lack Cys_{140}. The $Cys_{135}Cys_{139}Ala_{140}$ (k_{reox} = 0.16 min^{-1}) and $Ala_{135}Cys_{139}Cys_{140}$ (k_{reox} = 0.12 min^{-1}) enzymes which contain novel Cys pairs are intermediate in reoxidation rate.

Table VI: Multiple-Turnover Data for the $Ala_{135}Cys_{140}$ and $Ser_{135}Cys_{140}$ Mutant Mercuric Reductases. Reduction of Hg(II)–EDTA and $Hg(Cys)_2$ As Monitored by $^{203}Hg(0)$ Volatilization

enzyme and substrate	incubation time (min)	rate[a] (min^{-1})	turnovers (n)
$Ala_{135}Cys_{140}$			
Hg(II)–EDTA	240	0.14	34
Hg(II)–EDTA	360	0.090	33
$Hg(Cys)_2$	180	0.092	17
$Hg(Cys)_2$	420	0.077	32
$Ser_{135}Cys_{140}$			
Hg(II)–EDTA	240	0.12	28
Hg(II)–EDTA	360	0.10	37
$Hg(Cys)_2$	180	0.24	43
$Hg(Cys)_2$	420	0.14	58
$Cys_{135}Cys_{140}$ (wild type)			
$Hg(Cys)_2$		k_{cat} = 380 min^{-1} [b]	

[a] Rates are expressed as turnovers per minute per monomer. [b] This value, confirmed by the $^{203}Hg(0)$ volatilization assay, was previously reported by Fox and Walsh (1982).

Free $FADH_2$ can also be reoxidized at a rate of 0.30 min^{-1}, comparable to the mutants retaining Cys_{140}. Free FMN and riboflavin behave similarly. We have attempted to determine rate constants for reoxidation by $Hg(SR)_2$; however, in several cases we have been unable to see any reoxidation; in cases where reoxidation is observed, it occurs at rates significantly slower than those seen with Hg(II)–EDTA. This most likely reflects the more positive reduction potential of the Hg(II)/Hg(0) couple in the presence of EDTA as compared with thiols, which in turn derives from the differences in Hg(II) association constants characteristic for these two ligands (K_a for Hg(II)–EDTA $\approx 10^{22}$, K_a for $Hg(SR)_2 = 10^{38}$; Casas & Jones, 1980).

The above data clearly indicate that mutant mercuric reductases can proceed through at least one catalytic cycle although they do so at rates dramatically slower than that of the wild-type enzyme. Furthermore, these results with mutant enzymes lacking a redox-active disulfide mandate that Hg(II) reduction occurs via a reduced flavin intermediate. Mutant enzymes which retain Cys_{140}, the thiol closest to the flavin, reduce Hg(II) at rates 15–50-fold higher than the $Ala_{135}Ala_{140}$ mutant, which retains neither active site thiol. This may be due to binding of Hg(II) to Cys_{140} which would position the Hg(II) close to the flavin, thereby facilitating reduction by $FADH_2$.

Multiple Catalytic Turnovers of $Hg(SR)_2$ and Hg(II)–EDTA. To confirm the reduction of Hg(II) catalyzed by mutant mercuric reductases and to evaluate their ability to undergo multiple catalytic events, we have assayed the mutant enzymes using a ^{203}Hg volatility assay. In this assay using liquid scintillation counting, turnover is monitored, as $^{203}Hg(II)$ is converted to $^{203}Hg(0)$, by observing the loss of soluble radioactive $^{203}Hg(II)$ over time. Data for the $Ala_{135}Cys_{140}$ and $Ser_{135}Cys_{140}$ mutant enzymes are summarized in Table VI. Both mutants are clearly capable of multiple catalytic events. The maximal rate for Hg(II)–EDTA reduction observed is 0.14 min^{-1} for the $Ala_{135}Cys_{140}$ protein and 0.12 min^{-1} for the $Ser_{135}Cys_{140}$ enzyme. The highest reduction rate of $Hg(Cys)_2$ observed is 0.092 min^{-1} for the $Ala_{135}Cys_{140}$ enzyme and 0.24 min^{-1} for the $Ser_{135}Cys_{140}$ protein. These rates, while not identical, are similar to those measured in the single-turnover experiments. Differences in the single versus multiple turnover experiments may be related to the absence of nicotinamides in the former since pyridine nucleotide binding is known to modulate the redox behavior of many disulfide oxidoreductases. Additionally, it should be pointed out that Hg(0)

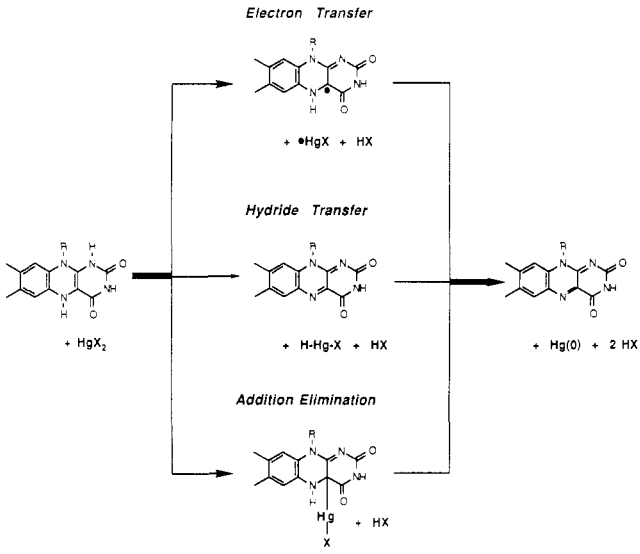

FIGURE 6: Three possible mechanisms for the reduction of Hg(II) by $FADH_2$.

produced is calculated by subtracting the $^{203}Hg(II)$ remaining at time t from the initial amount of $^{203}Hg(II)$ added to the reaction. To obtain reliable numbers, we have allowed the reaction to go to at least 40% completion, which means that the Hg(II) concentration has decreased significantly during the course of the reaction. Under such conditions our calculated rates will be underestimations of the initial velocity should the [Hg(II)] approach K_m concentrations, which are as yet undetermined in these experiments.

For the other mercuric reductase mutants, we have been unable to detect Hg(II) reduction. By direct explanation from the single-turnover data, the $Cys_{135}Ala_{140}$, $Cys_{135}Ser_{140}$, and $Ala_{135}Ala_{140}$ mutants would be predicted to reduce Hg(II) at approximately one-tenth the rate characteristic of the mutants discussed above. In our longest anaerobic turnover experiment, 7 h, such a rate could not have been detected.

Hg(II) Reduction by $FADH_2$. The results discussed above clearly demonstrate that the mechanism via which mutant mercuric reductases reduce Hg(II) involves a reduced flavin intermediate. Literature precedent exists for the reduction of Hg(II) by flavin semiquinone by an outer-sphere electron-transfer process (Singh, 1982). Our studies with free flavin extend these results by showing that $FADH_2$ can also function as a reductant.

Three possible mechanisms for the reduction of Hg(II) by $FADH_2$ are diagrammed in Figure 6. In addition to a possible electron-transfer mechanism, the alternatives include the reduction of Hg(II) via a hydride transfer from $FADH_2$ similar to that observed between metal hydride reagents and Hg(II) (Whitesides & San Filippo, 1970) and an addition–elimination mechanism involving Hg(II) addition to the C-4a position of $FADH_2$ followed by elimination of Hg(0) and the N-5 proton to yield oxidized flavin and reduced mercury. The addition–elimination pathway is essentially identical to the well-precedented mechanism of allylic oxidation of olefins by Hg(II) to yield metallic mercury and allylic alcohols or dienes (Rappoport et al., 1968, 1970; Fieser & Fieser, 1967). The mercuration of the $FADH_2$ C-4a–C-10a olefinic bond invoked in this mechanism also parallels the mercuration of the nicotinamide (Marshall et al., 1984) and uridine (Dale et al., 1975) heterocyclic systems, to which the flavin isoalloxazine is closely related. It should be noted that the examples discussed above all involve mercuration and subsequent reduction by $Hg(OAc)_2$ and $HgCl_2$. These compounds are substantially more reactive than $Hg(SR)_2$ and Hg(II)–EDTA, which are the substrates reduced by mercuric reductase; consequently, some caution may be necessary when extrapolating these mechanisms to these less reactive Hg(II) compounds.

In an attempt to distinguish between the above mechanisms, we have assessed the ability of 5-deazariboflavin to reduce Hg(II). 5-Deaza-FAD has been found to function as an effective replacement for FAD in enzymatic reactions involving hydride-transfer mechanisms (Walsh, 1986). Our results indicate that free 5-deaza-$FADH_2$ cannot reduce Hg(II) on a time scale of hours, suggesting that the mechanism of Hg(II) reduction by FAD does not occur by hydride transfer. This result is consistent with the addition–elimination mechanism since the C-5 proton in 5-deazariboflavin is substantially less acidic than its N-5 counterpart in FAD and consequently may not readily eliminate from a mercurated deazaflavin adduct, thus preventing flavin rearomatization and mercury reduction. It should be noted that the 5-deazaflavin results are also consistent with the electron-transfer mechanism.

Implications of Hg(II) Reduction by Mutant Mercuric Reductases. Mutant mercuric reductases lacking a complete redox-active disulfide were constructed to delineate the role of the $Cys_{135}Cys_{140}$ disulfide in catalysis. Our results clearly demonstrate two salient points concerning this. First, they implicate the $Cys_{135}Cys_{140}$ thiols in the binding of Hg(II) during catalysis. Additionally, they require that the catalytic reduction of Hg(II), observed for the mutant enzymes, occurs via a reduced flavin intermediate. It is possible that a similar mechanism is operable in the wild-type enzyme as well.

Given the extensive homology between mercuric reductase and glutathione reductase, it is tempting to envision a "homologous" mechanism in which Hg(II) reduction occurs through a pathway involving concomitant oxidation of the redox-active disulfide. While reduction of Hg(II) by thiols to yield Hg(0) and disulfide, as well as the reverse reaction, has been documented in the literature, these reactions occur only under specialized conditions such as on the surfaces of dropping mercury electrodes (Stankovich & Bard, 1977) or in high-energy photolysis reactions (Kern, 1958; Brandt et al., 1952), which require the presence of highly reactive thiyl radicals (Caspari & Granzow, 1970).

While some investigators have observed oxidation of thiols to disulfides in the presence of Hg(II), they have clearly shown that these results derive from a catalytic effect of Hg(II) on the oxidation of thiols by molecular oxygen similar to that observed with Fe(III), Cu(II), and Ni(II) (Cullis et al., 1968). Electrochemical experiments conducted by Stankovich and Bard (1977) using cyclic voltammetry with a hanging drop mercury electrode also indicate that an RSSR bond is not formed upon oxidation of cysteine in the presence of Hg(II). In short, we have found no examples of the preparative use of thiols to reduce Hg(II); instead, the chemistry between thiols and Hg(II) in aqueous solution is dominated by the formation of bidentate mercaptides (Torchinsky, 1981) whose structures are known crystallographically (McAuliffe, 1977). In the presence of excess thiols, ligand exchange via attack of a thiolate anion on the strongly electropositive metal center occurs (Rabenstein, 1978) in lieu of reduction. The reactivity of Hg(II) toward thiols is summarized in Scheme I. While the lack of precedent for Hg(II) reduction by thiols does not prove that the reaction cannot occur, it seems unlikely that this previously undetected chemistry is operating in mercuric reductase.

In contrast to the thiol/mercury redox mechanism described above, the reduction of Hg(II) by $FADH_2$ has substantially

Scheme I

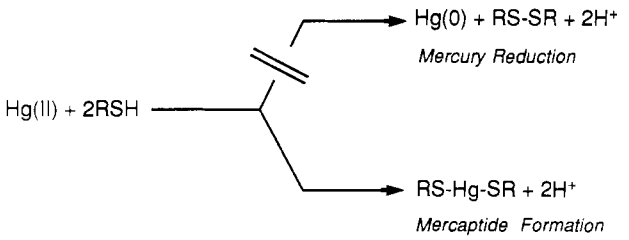

better precedent. In addition to our observation of Hg(II) reduction by $FADH_2$ and that of Singh et al. (1982) concerning the reduction of Hg(II) by flavin semiquinone, there are a variety of examples of oxidation of activated olefinic systems (similar to the C-4a–C-10a locus in $FADH_2$ noted in Figure 6) by Hg(II) to yield Hg(0). Thus the reduction of Hg(II) by $FADH_2$, as was directly observed with the mutant mercuric reductases, appears to be the more likely pathway for reduction in the wild-type enzyme.

Earlier investigations of wild-type mercuric reductase employing stopped-flow spectrophotometry have demonstrated that the EH_2 and EH_2–$NADP^+$ forms of the enzyme appear kinetically incompetent (Miller et al., 1986). Additional experiments detected the EH_2–NADPH form (a formal EH_4 equivalent) in steady-state turnover experiments, which was then suggested to be the catalytically active form (Sahlman et al., 1984). In contrast to the EH_2 and EH_2–$NADP^+$ forms, the EH_2–NADPH complex retains an additional complement of two electron equivalents and thus represents a species of higher reducing power. More specifically, it is a possible progenitor of an EH_4–$NADP^+$ complex, which would possess both a reduced disulfide to act as a Hg(II) binding site as well as the reduced flavin we postulate to be the actual Hg(II) reductant.

The EH_4 form of wild-type mercuric reductase can only be observed in spectrophotometric titration experiments of enzyme with nicotinamides at pH <6 (Sahlman et al., 1986). Although some of the EH_4 species may be present at pH >6, unequivocal assignment is complicated by the perturbing effects of nicotinamides on the flavin spectrum. Detailed experiments with the EH_2 form of *E. coli* lipoamide dehydrogenase using a combination of spectrophotometric and fluorescence spectroscopy did reveal a reduced flavin component present even in the two-electron-reduced form (Wilkinson & Williams, 1979a); however, the requisite fluorescence experiments have not been performed on mercuric reductase.

For mutant mercuric reductases, titration of the $Ala_{135}Cys_{140}$ mutant at pH 7.3 with NADPH gives results similar to those for wild-type EH_2 where essentially no $FADH_2$ is observed. By contrast, in analogous experiments with the $Cys_{135}Ala_{140}$ and $Ala_{135}Ala_{140}$ mutant proteins, considerable $FADH_2$ character is observed. It is likely that the absence of discernible reduced flavin species in the NADPH titrations of both the wild-type EH_2 and the $Ala_{135}Cys_{140}$ enzymes reflects the influence of the charge-transfer interaction on the FAD/$FADH_2$ reduction potential. This interaction, which selectively stabilizes the oxidized flavin form, requires a thiolate anion whose concentration is pH dependent; thus protonation at lower pH results in the disruption of the charge-transfer complex, which in turn facilitates EH_2 reduction to EH_4 (Sahlman et al., 1986), as is observed in the wild-type enzyme. It should be noted that binding of a Lewis acid such as Hg(II) to the Cys_{140} charge-transfer thiolate in lieu of protonation should result in a decrease in charge-transfer absorbance with concomitant reduction of the FAD. This has been observed with wild-type EH_2 (Miller et al., 1987) as well as with the $Ala_{135}Cys_{140}$ mutant protein (data not shown); such binding of Hg(II) may occur in the catalytic cycle of wild-type mercuric reductase.

Scheme II: Proposed Catalytic Cycle for Wild-Type Mercuric Reductase

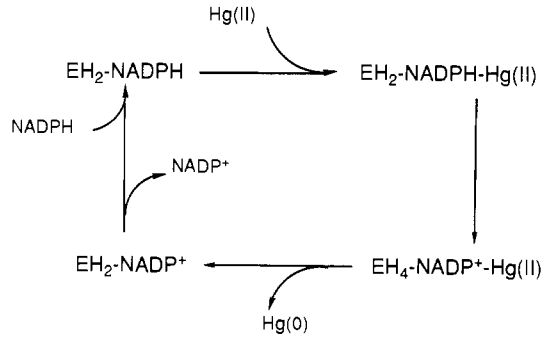

Despite our inability to directly observe any accumulating EH_4 species in wild-type mercuric reductase under turnover conditions, we believe that such species are important catalytic intermediates and that substantial evidence exists to support this hypothesis. First, we note that, in addition to reducing Hg(II), mercuric reductase also catalyzes transhydrogenation reactions and reduces molecular oxygen. There can be little doubt that the latter two activities require the existence of a reduced flavin intermediate. Although for wild-type mercuric reductase such a reduced flavin may result from a two-electron-reduced species, which contains $FADH_2$ and oxidized disulfide, this appears unlikely for two reasons. First, alkylation of Cys_{135} with iodoacetamide which eliminates the redox-active disulfide (this species is termed EHR) results in a 2.5-fold *increase* in the transhydrogenase k_{cat} (Fox & Walsh, 1983). In the case of this modified form of mercuric reductase, transhydrogenation can only occur through a reduced flavin (EH_4-like) species. We also note that the resulting rate of transhydrogenation for EHR (225 min^{-1}) is of similar magnitude as the value for Hg(II) reduction (380 min^{-1}) catalyzed by the wild-type enzyme.

In this paper we have presented substantial evidence that mutant mercuric reductases, which lack a redox-active disulfide, reduce oxygen and transhydrogenate through an obligatory reduced flavin intermediate despite the fact that some of their reduction potentials at pH 7 are more negative than the NADPH/$NADP^+$ redox couple. We have noted above that, with the mutant enzymes, there is a correlation between E-FAD/E-$FADH_2$ reduction potential and the transhydrogenation and oxygen reduction activities. Such a correlation may, in fact, reflect the actual concentration of catalytically competent reduced flavin intermediate present. We note that the k_{cat} values for transhydrogenation and oxygen reduction for wild-type enzyme correlate substantially better when the EH_2/EH_4 reduction potential rather than the E/EH_2 value is used. This in turn suggests that the wild-type protein performs these catalytic activities by cycling between the EH_2 and EH_4 (reduced flavin) forms. If such reduced flavin species participate in transhydrogenation and oxygen reduction, it is possible that they can also function during Hg(II) reduction.

On the basis of the results discussed above, a scheme that delineates the enzyme species relevant to the catalytic cycle of wild-type mercuric reductase is presented in Scheme II. In this pathway we propose that the viable reducing species is an EH_4–$NADP^+$–Hg(II) complex and that the actual reductant in that species is $FADH_2$. This model, which utilizes the enzyme thiols for Hg(II) binding followed by reduction by $FADH_2$, closely parallels the electrochemical reduction of $Hg(SR)_2$ bound at the mercury electrode as elaborated by

Stankovich and Bard (1977). The mutagenesis results presented here also provide evidence that the enzyme-bound Hg(II) is liganded to the active site thiols; but these results alone do not indicate the complete nature of the Hg(II) complex. In the following papers (Moore & Walsh, 1989; Miller et al., 1989) evidence is given that additional enzyme-derived ligands are essential for binding Hg(II) at the active site in the normal, rapidly reducible configuration.

Summary. We have constructed mutant mercuric reductases lacking a redox-active disulfide, which reduce Hg(II) through discrete reduced flavin intermediates at rates ca. 1000-fold slower than that of the wild-type enzyme. These results also implicate the Cys_{135} and Cys_{140} thiols in a Hg(II) binding role and suggest a possible mechanism for mercuric ion reduction by the wild-type enzyme that involves reduced flavin. Additional experiments to confirm the existence of an EH_4 species under catalytic conditions, as well as experiments to examine the binding of Hg(II) to the enzyme under similar conditions, are necessary to substantiate our hypothesis. In the event that reduced flavin intermediates are not involved in Hg(II) reduction by wild-type mercuric reductase, model chemistry for Hg(II) reduction by thiols must be developed.

ACKNOWLEDGMENTS

We thank V. Massey, S. Miller, D. Ballou, and C. Williams for their determinations of the $Ser_{135}Cys_{140}$ and $Cys_{135}Ser_{140}$ reduction potentials, for providing details of the xanthine–xanthine oxidase procedure for determining reduction potentials, and for valuable advice and discussion. We thank O. Ploux for generously providing the (4*S*)-[4-^{2}H]NADPH used in the kinetic isotope experiments. We thank B. Fox for the determination of the wild-type FAD K_m. We also thank M. Moore, P. Schultz, S. Shames, T. Begley, and members of the Walsh group for helpful discussions during the course of this work.

Registry No. Cys, 52-90-4; Ala, 56-41-7; Gly, 56-40-6; NADPH, 53-57-6; FAD, 146-14-5; mercuric reductase, 67880-93-7; cystine, 56-89-3.

REFERENCES

Abramovitz, A. S., & Massey, V. (1976) *J. Biol. Chem. 251*, 5327.

Arscott, L. D., Thorpe, C., & Williams, C. H. (1981) *Biochemistry 20*, 1513.

Brandt, G., Emeleus, H. J., & Haszeldine, R. N. (1952) *J. Chem. Soc.*, 2198.

Brown, N., Ford, S., Pridmore, R., & Fritzinger, D. (1983) *Biochemistry 22*, 4089–95.

Brown, R. D., & Rogers, E. F. (1978) *Biochemistry 17*, 1942.

Capasso, S., Mattia, C., Mazzarella, L., & Puliti, R. (1977) *Acta Crystallogr. B33*, 2080.

Casas, J. S., & Jones, M. M. (1980) *J. Inorg. Nucl. Chem. 42*, 99.

Caspari, G., & Granzow, A. (1970) *J. Phys. Chem. 74*, 836.

Cleland, W. W. (1975) *Biochemistry 14*, 3220.

Cullis, C. F., Hopton, J. D., Swan, C. J., & Trimm, D. L. (1968) *J. Appl. Chem. 18*, 335.

Dale, R. M. K., Martin, E., Livingston, D. J., & Ward, D. C. (1975) *Biochemistry 14*, 2447.

Dixon, M., & Kenworthy, P. (1967) *Biochim. Biophys. Acta 146*, 54.

Fieser, L. F., & Fieser, M. (1967) *Reagents for Organic Synthesis*, p 644, Wiley, New York.

Fox, B., & Walsh, C. (1982) *J. Biol. Chem. 257*, 2498.

Fox, B., & Walsh, C. (1983) *Biochemistry 22*, 4082.

Gerstein, J., & Jencks, W. P. (1964) *J. Am. Chem. Soc. 86*, 4655.

Kao, P. N., & Karlin, A. (1986) *J. Biol. Chem. 261*, 8085.

Kern, R. J. (1953) *J. Am. Chem. Soc. 75*, 1865.

Kunkel, T. A. (1984) *Proc. Natl. Acad. Sci. U.S.A. 81*, 1494.

Laemmli, U. K. (1970) *Nature 227*, 680.

Light, D. R., & Walsh, C. (1980) *J. Biol. Chem. 255*, 4264.

Lowry, O. H., Rosebrough, N. J., Farr, A. L., & Randall, R. J. (1951) *J. Biol. Chem. 193*, 265.

Maniatis, T., Fritsch, E. F., & Sambrook, J. (1982) *Molecular Cloning: A Laboratory Manual*, Cold Spring Harbor Laboratory, Cold Spring Harbor, NY.

Marshall, J. L., Booth, J. E., & Williams, J. W. (1984) *J. Biol. Chem. 259*, 3033.

Matthews, R. G., & Williams, C. T. (1976) *J. Biol. Chem. 251*, 3956.

McAuliffe, (1977) *The Chemistry of Mercury*, p 79, Macmillan, London.

Miller, S. M., Massey, V., Ballou, D. P., Williams, C. H., & Walsh, C. (1986) *J. Biol. Chem. 261*, 8081.

Miller, S. M., Massey, V., Ballou, D. P., Williams, C. H., Moore, M., & Walsh, C. (1988) *Flavins and Flavoproteins: Procedings of the Ninth Symposium on Flavins and Flavoproteins* (in press).

Miller, S. M., Moore, M. J., Massey, V., Williams, C. H., Jr., Distefano, M. D., Ballou, D. P., & Walsh, C. T. (1989) *Biochemistry* (third of three papers in this issue).

Mills, D. R., & Kramer, F. R. (1979) *Proc. Natl. Acad. Sci. U.S.A. 76*, 2232.

Moore, M. J., & Walsh, C. T. (1989) *Biochemistry* (second of three papers in this issue).

Pai, E. F., & Schulz, G. E. (1983) *J. Biol. Chem. 258*, 1752.

Rabenstein, D. L. (1978) *Acc. Chem. Res. 11*, 100.

Rappoport, Z., Sleezer, P. D., Winstein, S., & Young, W. G. (1965) *Tetrahedron Lett.*, 3719.

Rappoport, Z., Dyall, L. K., Winstein, S., & Young, W. G. (1970) *Tetrahedron Lett.*, 3483.

Rinderle, S. J., Booth, J. E., & Williams, J. W. (1983) *Biochemistry 22*, 869.

Rivlin, R. S. (1975) *Riboflavin*, pp 4–5, Plenum Press, New York.

Sahlman, L., Lambier, A.-M., Lindskog, S., & Dunford, H. B. (1984) *J. Biol. Chem. 259*, 12403.

Sahlman, L., Lambeir, A.-M., & Lindskog, S. (1986) *Eur. J. Biochem. 156*, 479.

Sanger, F., Coulson, A. R., Barrell, B. G., Smith, A. J. H., & Roe, B. A. (1981) *J. Mol. Biol. 143*, 161.

Schottel, J. L. (1978) *J. Biol. Chem. 253*, 4341.

Schulz, G., Schirmer, R., Sachsenheimer, W., & Pai, E. (1978) *Nature 273*, 121.

Schulz, P., Au, K., & Walsh, C. (1985) *Biochemistry 24*, 6840–8.

Singh, A. N., Gelerinter, E., & Gould, E. S. (1982) *Inorg. Chem. 21*, 1232.

Stankovich, M. T., & Bard, A. J. (1977) *J. Electroanal. Chem. 75*, 487.

Stewart, R. C., & Massey, V. (1985) *J. Biol. Chem. 260*, 13639.

Summers, A. (1986) *Annu. Rev. Microbiol. 40*, 607–34.

Torchinsky, Y. M. (1981) *Sulfur in Proteins*, pp 41–46, Pergamon, New York.

Walsh, C. (1986) *Acc. Chem. Res. 19*, 216.

Walsh, C., Fisher, J., Spencer, R., Graham, D. W., Ashton, W. T., Brown, J. E., Brown, R. D., & Rogers, E. F. (1978) *Biochemistry 17*, 1942.
Whitesides, G., & San Filippo, J. (1970) *J. Am. Chem. Soc. 92*, 6611–24.
Wilkinson, K., & Williams, C., Jr. (1979a) *J. Biol. Chem. 254*, 852–62.
Wilkinson, K., & Williams, C., Jr. (1979b) *J. Biol. Chem. 254*, 862–71.
Williams, C. H. (1976) *Enzymes (3rd Ed.) 13*, 89.
Williams, C. H., Arscott, D. L., Matthews, R. G., Thorpe, C., & Wilkinson, K. D. (1979) *Methods Enzymol. 62D*, 185.
Williams, C. H., Arscott, D. L., & Schulz, G. (1982) *Proc. Natl. Acad. Sci. U.S.A. 79*, 2199.
Wilson, G. S. (1978) *Methods Enzymol. 54*, 396.
Zoller, M. J., & Smith, M. (1986) *Methods Enzymol. 100*, 468.
Zoller, M. J., & Smith, M. (1984) *DNA 3*, 479.

Mutagenesis of the N- and C-Terminal Cysteine Pairs of Tn*501* Mercuric Ion Reductase: Consequences for Bacterial Detoxification of Mercurials†

Melissa J. Moore and Christopher T. Walsh*
Department of Biological Chemistry and Molecular Pharmacology, Harvard Medical School, Boston, Massachusetts 02115
Received June 1, 1988; Revised Manuscript Received September 20, 1988

ABSTRACT: Mercuric ion reductase (the *merA* gene product) is a unique member of the class of FAD and redox-active disulfide-containing oxidoreductases by virtue of its ability to reduce Hg(II) to Hg(0) as the last step in bacterial detoxification of mercurials. In addition to the active site redox-active disulfide, formed between Cys_{135} and Cys_{140} in Tn*501* MerA, the protein products of the three *merA* gene sequences published to date have two additional conserved pairs of cysteines, one near the N-terminus ($Cys_{10}Cys_{13}$ in Tn*501* MerA) and another near the C-terminus ($Cys_{558}Cys_{559}$ in Tn*501* MerA). Neither of these pairs is found in other members of this enzyme family. To assess the possible roles of these peripheral cysteines in the Hg(II) detoxification pathway, we have constructed and characterized one single mutant, $Cys_{10}Ala_{13}$, and two double mutants, $Ala_{10}Ala_{13}$ and $Ala_{558}Ala_{559}$. The N-terminal mutants are fully functional in vivo as determined by $HgCl_2$ resistance studies, showing the N-terminal cysteine pair to be dispensable. In contrast, the $Ala_{558}Ala_{559}$ mutant is defective for $HgCl_2$ resistance in vivo and $Hg(SR)_2$ reduction in vitro, thereby implicating Cys_{558} and/or Cys_{559} in Hg(II) reduction by the wild-type enzyme. Other activities, such as NADPH/thio-$NADP^+$ transhydrogenation, NADPH oxidation, and DTNB reduction, are unimpaired in this mutant.

Mercuric reductase is the flavoenzyme that catalyzes the last and crucial step in Hg(II) detoxification by bacteria [for review see Foster (1983) and Summers (1986)]:[1]

$$Hg(SR)_2 + NADPH + H^+ \rightarrow Hg(0) + NADP^+ + 2HSR$$

It shows strong active site similarity to the disulfide oxidoreductases, pig heart lipoamide dehydrogenase, human glutathione reductase, and trypanothione reductase (Fox & Walsh, 1983; Shames et al., 1986), which catalyze the flow of electrons from NAD(P)H to disulfide substrates via a flavin coenzyme and an active site redox-active disulfide. However, while the three former proteins are all capable of binding mercurials in their two-electron-reduced states (Massey & Williams, 1965; Casola & Massey, 1966; Miller et al., 1986), only mercuric reductase is able to catalyze reduction of Hg(II) at a useful rate. In contrast, the physiological activities of both glutathione reductase and lipoamide dehydrogenase are potently inhibited by mercurials.

Tn*501* mercuric reductase is encoded by the *merA* gene of the *mer* operon in transposon Tn*501*, originally isolated on a plasmid from *Pseudomonas aeruginosa* (Stanisich et al., 1977). This operon is composed of a regulatory gene, *merR*, an operator/promoter region, and four structural genes: *merT*, *-P*, *-A*, and *-D*. *merT* and *merP* encode Hg(II)-transport and periplasmic Hg(II)-binding proteins, respectively, while no definitive function has yet been assigned to *merD*. A recurring structural motif throughout these *mer* gene products is the

Table I: Primary-Sequence Cysteine Pairs in the Tn*501* *mer* Operon

MerR[a]	113-LeuValCysAlaCysHisAla-119
MerT[b]	21-AlaSerAlaCysCysLeuGly-27
	76-CysLysProGlyGluValCys-82
MerP[b]	31-MetThrCysAlaAlaCysPro-37
MerA[c]	8-MetThrCysAspSerCysAla-14
	134-ThrCysValAsnValGlyCys-140
	555-GlnLeuSerCysCysAlaGly-561

[a] O'Halloran & Walsh, 1987. [b] Misra et al., 1984. [c] Brown et al., 1983.

† This work was supported in part by NIH Grant GM 216439. M.J.M. was the recipient of a National Science Foundation Predoctoral Fellowship.
* To whom correspondence should be addressed.

[1] Abbreviations: NADPH, reduced nicotinamide adenine dinucleotide phosphate; thio-$NADP^+$, thionicotinamide adenine dinucleotide phosphate; FAD, flavin adenine dinucleotide; DTNB, 5,5′-dithiobis(2-nitrobenzoate); TNB, 5-thio-2-nitrobenzoate dianion; EDTA, ethylenediaminetetraacetic acid; IPTG, isopropyl β-D-thiogalactopyranoside; bp, DNA base pair(s); SDS, sodium dodecyl sulfate; PAGE, polyacrylamide gel electrophoresis; HPLC, high-performance liquid chromatography; N or C terminal, proximal to the amino or carboxyl terminus of a protein; E_{ox}, EH_2, and EH_4, oxidized, two-electron-reduced, and four-electron-reduced forms, respectively, of mercuric reductase or of the disulfide oxidoreductases; K_{si}, inhibition constant for binding of a second substrate molecule to the enzyme–substrate complex.

0006-2960/89/0428-1183$01.50/0